GPS Precise Tracking Of Topex/Poseidon: Results and implications

W. I. Bertiger, Y. E. Bar-Sever, E. J. Christensen, E. S. Davis, J. R. Guinn, B. J. Haines, R. W. Ibanez-Meier, J. R. Jet, S. M. Lichten, W. G. Melbourne, R. J. Muellerschoen, T. N. Munson, Y. Vigue, S. C. Wu, and T. P. Yunck
of the
Jet Propulsion Laboratory, California Institute of Technology

B. E. Schutz, P. A. M. Abusali, H. J. Rim, M. M. Watkins
of the
Center for Space Research, University of Texas

P. Willis
of the
Institute Geographique National, France

Submitted for Publication to *JGR* TOPEX/Poseidon Special Issue, Nov 1993

GPS Precise Tracking Of Topcx/Poseidon: Results and Implications

W. 1. Bertiger, Y. F. Bar-Sever, E. J. Christensen, E . S. Davis, J. R. Guinn, B. J. Haines, R. W. Ibanez-Meier, J. R. Jcc, S. M. Lichten, W. G. Melbourne, R. J. Muellerschoen, T. N. Munson, Y. Vigue, S. C. Wu, and T. P. Yunck
of the
Jet Propulsion Laboratory, California Institute of Technology

B. E. Schutz, P. A. M. Abusali, H. J. Rim, M. M. Watkins
of the
Center for Space Research, University of Texas

1'. Willis
of the.
Inst it ute Geographique National, France

ABSTRACT

A "reduced dynamic" filtering strategy that exploits the unique geometric strength of the Global Positioning System to minimize the effects of force model errors has yielded orbit solutions for TOPEX/Poseidon which appear accurate. to better than 3 cm (1 σ) in the. radial component. Reduction of force 1I1O(1CI error also reduces the geographic correlation of the orbit error. With a traditional dynamic approach, GPS yields radial mbit accuracies of about 5 cm, comparable to the accuracy delivered by satellite laser ranging and the. DORIS Doppler tracking system. A portion of the. dynamic orbit error is in the JGM-2 gravity model; GPS data from TOPEX/Poseidon can readily reveal that error' ant] have been used to improve the gravity model. The operational aspects of a precise. GPS tracking system have also been assessed. The I'ol'led}'oscidon experience suggests that automated GPS techniques can bring the cost of precise orbit determination well under that of conventional tracking systems.

INTRODUCTION

in the mid- 1980s the TOPEX/Poseidon Project (Fu et al., this issue) agreed to develop and fly an experimental Global Positioning System receiver to test the ability of GPS to provide precise orbit determination (POD) by an unconventional new technique (Melbourne et al., 1994). The GPS receiver aboard TOPEX/Poseidon tracks the dual L-band radio signals from a constellation of 24 GPS satellites, collecting navigation data from up to six satellites at once. Since the orbits and clock offsets of the GPS satellites are known (they are broadcast by the GPS satellites) the receiver can determine its position and time (four unknowns) geometrically at any instant with data from only four satellites. It is this extraordinary geometric strength that distinguishes GPS as a tracking system. Such ground-based systems as SLR (satellite laser ranging) and DORIS (Doppler Orbitography and Radio positioning integrated by Satellite) typically provide measurements in just one direction at a time and may have substantial coverage gaps; they must therefore rely on models of satellite trajectories (derived from models of the forces acting on the satellite) to recover 3-D information.

With a technique known as reduced dynamic tracking (Wu et al., 1991; Yunck et al., 1990, 1994) we can exploit the 3-D geometric strength of GPS to minimize dependence on dynamic models and, in theory, achieve a superior orbit solution through an optimal synthesis of dynamic and geometric information. A variation on that technique called kinematic tracking can yield a precise solution almost entirely by geometric means.

Conventional dynamic POD depends on precise models of the forces acting, on the satellite to describe the trajectory. in a dynamic solution the estimated parameters will typically include the satellite initial state (position and velocity) and a few quantities describing the force models (e.g., a drag coefficient). These are adjusted to yield a solution that best fits the observations, but that solution will necessarily have errors arising from errors in the force models. With GPS tracking, the model errors can be observed in the 3-D residuals between the orbit solution and the observations. This residual information can then be applied in a point-by-point geometric adjustment of the satellite position to give the reduced dynamic solution (Fig. 1). Differences between dynamic and reduced dynamic solutions can expose the model errors and allow us to study their geographical and spectral distribution. Alternatively, parameters describing the gravity field can be adjusted in a dynamic GPS solution to improve (or tune) the gravity model with an unprecedented degree of global strength.

Institutional Roles

This work involved a collaboration between groups at the Jet Propulsion Laboratory (JPL), the Center for Space Research (CSR) of the University of Texas at Austin, and a scientist visiting JPL, from the Institut Geographique National (IGN) in Paris. The JPL team focused on refining the reduced dynamic strategy, while CSR, which has long experience in dynamic estimation with SLR, adapted their software for dynamic POD and gravity tuning with GPS data (Rim, 1992). Although the JPL and CSR analysis systems were developed independently (Wu et al., 1990; Webb et al., 1993; Rim, 1992), they share some common models. Comparisons between orbits produced with each system serve as an important validation test.

IGN has expertise in the DORIS system and worked closely with JPL to adapt JPL's analysis software to process DORIS data. CSR modified its software independently to process DORIS data as well (Watkins et al., 1992). In addition, complementary efforts are underway at the Goddard Space Flight Center (GSFC) and CNES (Centre National d'Etudes Spatiale) in Toulouse to produce the official precise orbits with SLR and DORIS data (Tapley et al., this issue).

Experiment Goals

The major goals of the GPS Experiment are. to (1) evaluate the accuracy and operational potential of GPS for tracking Earth satellites; (2) provide. a data base that includes the GPS-based orbit solutions, calibration data, and reference frame tics for post-experiment use by the Project (Born et al., this issue; Christensen et al., this issue); and (3) provide production GPS POD technology for possible conversion to an operational system.

in the 1980s, covariance analysis suggested that an accuracy of 5 to 10 cm might be achieved if data from 6 globally distributed GPS ground receivers were used together with the. flight data to solve for the TOPEX/Poseidon orbit (Wu and Ondrasik, 1 982; Yunck and Wu, 1986; Wu et al., 1987). We there.fore adopted "better than 10 cm RMS in altitude" as a formal goal for the experiment. Analysis further showed that ionospheric calibration with dual frequency GPS data would also be needed. We should note that the. flight receiver developed for the experiment can not receive both frequencies when the GPS security feature known as anti-spoofing (AS) is active, It was therefore necessary to arrange. with the Department of Defense (DoD) to have AS off for nine 1()-clay periods in the first year of the mission to ensure an adequate data set for analysis. Future receiver designs could avoid this problem by adopting, either a GPS decryption capability or advanced codeless tracking technique.s.

Our objective in evaluating the operational potential the GPS POD system is to see if GPS can be a cost-effective alternative to existing precise tracking systems. Measures of operational performance include time delay in producing and validating the precise orbit products, reliability of the system, and cost of operation.

Recognizing the potential to support the TOPEX/Poseidon Project more formally, we also set out to 1) collect, edit and archive all data over the experiment lifetime (1 year for the flight receiver & 2 years for the ground network); 2) tune the gravity model to improve, the ocean geoid at wavelengths >1000 km; and 3) make available to the Project the most precise. orbits for use in oceanographic studies and for altimetric calibration at the verification sites.

SYSTEM DESIGN

The GPS tracking system consists of four segments: the. GPS constellation, the flight receiver, a global network of GPS ground receivers, and a central monitor, control and processing facility (Fig. 2). The POD strategy requires continuous tracking of the visible GPS satellites by ground and flight receivers. Data from all receivers arc. brought together and processed in a grand solution in which the TOPEX/Poseidon orbit, all GPS orbits, receiver and transmitter clock offsets, carrier phase biases, and a number of other parameters are estimated. Simultaneous sampling at all receivers (which may be achieved by later interpolation) eliminates common errors, such as clock dithering, which is a feature of another GPS security feature, known as selective availability (SA). In the end, TOPEX/Poseidon position and velocity are determined in a reference frame established by key sites in the global network; those sites are known absolutely with respect to the geocenter to about 2 cm in (he. International Terrestrial Reference Frame.

The Global Positioning System

Figure 3 depicts the GPS constellation, which is controlled from Falcon AFB near Colorado Springs. The constellation consists of 24 GPS satellites in 12-hoLll (20,200 -km altitude) circular orbits (Milliken and Zoller, 1978; Spilker, 1978). The satellites are. distributed in six orbit planes inclined at 55°, with a nodal separation of 60°. Each satellite broadcasts navigation signals on two L-band frequencies: 1.57542 GHz (L1) and 1.2276 GHz (L2). The corresponding carrier wavelengths arc approximately 19 and 24 cm. The two frequencies are used to calibrate the ionospheric delay. The beamwidths of the GPS signals extend roughly 3,000 km beyond the limb of the earth as viewed from the GPS satellites. At any point on the earth's surface, or in the space below 3000 km, typically 5 to 9 GPS satellites are continuously visible within a vertically centered hemispherical field of view. Each L-band carrier is modulated with a precise pseudo-random ranging code known as the P-code. The receiver measures precisely and unambiguously the arrival time of each code bit since the transmit time (according to the transmitter clock) of each bit is known, this gives a measure of the pseudorange. Each satellite broadcasts a unique code orthogonal to the others, enabling separation of the received GPS signals. The L1 signal is also modulated in quadrature (90° out of phase from the P-code) by a less precise ranging code known as the coarse/acquisition or C/A-code. Finally, both L-band signals are further modulated by a 50 bit/sec data message, which provides accurate GPS orbits, clock offsets from a time standard known as GPS time, satellite health status, and other information of value to the user. For precise applications dual-band carrier phase measurements, which are recovered by the receiver as part of its code tracking operations, are the primary GPS data type.

Pseudorange is the range between the phase centers of the GPS satellite and receiver antennas, plus the offset between the transmitter and receiver clocks. The pseudorange measurement, however, is corrupted by various other errors. The ground receivers, for example, see an additional delay caused by the earth's atmosphere. After the ionospheric delay has been removed by dual-frequency combination, carrier phase measures the same quantity as pseudorange, with two distinct differences: it is about one hundred times more precise and it has an arbitrary bias resulting from the unknown number of whole cycles between the transmitter and receiver and from various instrumental biases. The ionosphere-free observables are given, in simplified form, by

$$pseudorange = range + clock\_offset + troposphere + noise$$

$$carrier\_phase = range + clock\_offset + troposphere + bias$$

$$+ \textit{small\_noise} \quad [2]$$

A more detailed description is given by Wu et al. (1990).

The GPS Flight Receiver.

Figure 4 is a sketch of the TOPEX/Poseidon spacecraft, showing the locations of some subsystems and flight instruments. The GPS antenna is atop a 4.3-m mast, above the main body of the satellite, to suppress reflected signals from the TDRS high-gain antenna and other prominent surfaces. The GPS Demonstration Receiver (GPSDR), an early version of the. Motorola Monarch™ (not visible) tracks up to six GPS satellites concurrently, measuring the phase of each carrier at 1-sec intervals and pseudorange at 10-sec intervals. Measurement noise on the ionosphere-free observables, including instrumental thermal noise and multipath effects, is about 5 mm for phase and 70 cm for pseudorange. For details on the flight receiver see Zieger et al, (1994).

The Global Tracking Network.

Figure 5 shows the primary ground sites used in the experiment. These wil be part of the International GPS Service (IGS) set to begin providing high accuracy GPS data products to scientific users in 1994, under the auspices of the international Association of Geodesy (Neilan et al., 1993). For TOPEX/Poseidon fewer than a dozen sites are needed to obtain full accuracy because of the. ample common GPS visibility between the satellite ant] the ground sites. For GPS ground programs (which now achieve a weekly geocentric station location precision of about 1 cm), 20-40" sites are sometimes required (Blewitt et al., 1993).

The GPS Operations Center

All transactions involving GPS data and POD products flow through the operations center, which automatically retrieves data from a]] GPS sources-- about 8 Mbyte/day from the flight receiver and] Mbyte/day from each ground site. The center monitors and controls the ground and flight receivers and initiates actions to repair system faults. The Rogue™ and Turbo-Rogue™ ground receivers can store their data for, in most cases, up to 12 days to protect against communication outages. in the first 6 months of experimental operations we acquired 99% of the possible data from the flight receiver when GPS anti-spoofing was off, and about 95% from the ground receivers.

Precise GPS-based mbits for TOPEX/Poseidon are now produced at J} '1. with 30-hr data arcs on *2.4-h'* centers, providing 6-hr Over] aps for compari sons. '1'hose orbits and statistical qualit y measures arc available about 8 hrs after all data for a 30-hr arc arc received. External release of the. orbits occurs about 3 clays after the end of each 10-day mbit repeat cycle. Processing of the orbits is automated and data driven. Once the analysis process is initiated on the workstation it runs continuously, around the clock, with no operator attention except to deal with rare. anomalies. The process wakes up every 3 hrs to see if the data for a given arc have arrived. When the required data are there, processing for a 30-hr arc begins.

SOLUTION STRATEGIES

Here wc compare TOPEX/Poseidon precise orbits computed by three groups: JPL, CSR, and GSFC. Each group used different anal ysis soft ware. applied to one or more of three. precise tracking data types: G] 'S, DORIS and SLR. GSFC employs a combination of SLR and DORIS data to deliver operationally the precise orbits placed on the official Geophysical Data Records (GDRs) distributed to scientists (Tapley et al., this issue). JPL and CSR have performed experimental analysis of the GPS data, and have analyzed some combination of SLR ant] DORIS data as well. While their orbit estimation techniques differ in important ways, the three groups share common models for TOPEX/Poseidon dynamics and for the positions of observing (or transmitting) points on the earth relative to inertial space, in which the orbit is propagated. JPL's strategy is unique among the three in its use of Kalman filtering and stochastic models to permit reduced dynamic orbit determination.

TOPEX/Poseidon Dynamic Models

While the analysis systems share common dynamic models, those models are realized through implementations which give slight differences in the computed ocean tides and earth albedo (Tapley et al., this issue). All solutions, unless otherwise noted, use the JGM-2 gravity field tuned with TOPEX/Poseidon SLR and DORIS data (Lerch et al., 1993; Nerem et al., this issue), A custom model for the solar and the.rma] radiation forces on TOPEX/Poseidon was developed for the SLR/DORIS effort (Marshal et al., 1 992). The thermal radiation portion of the model was not used in the JP1. GPS solutions, however. These small, slowly varying dynamic model differences can be largely accommodated through the adjustment of an empirical acceleration parameter, $\ddot{a}$, of the form

$$\ddot{a} = \ddot{C} + \sum_{i=1}^{2} \ddot{A}_i \cos\omega_i t + \ddot{B}_i \sin\omega_i t \qquad [3]$$

where $\ddot{C}$, $\ddot{A}_i$, and $\ddot{B}_i$ are constant vectors in the spacecraft coordinate system oriented in the nominal along-track and cross-track directions (Kaplan, 1 976). The frequencies ω_i are once- and twice-per-revolution of TOPEX/Poseidon and t is time past an epoch. Solutions produced by CSR (with UTOPIA and MSODP1) and GSFC (with Geodyn) adjusted constant and once-per-rev along-track and cross-track amplitudes, while JPL's preliminary dynamic solutions (with GIPSY/OASIS 11) adjusted twice-per-rev terms in those components as well.

GPS Dynamic Model

The dynamic model for the GPS satellites contains only two components: the JGM-2 gravity field up to degree and order 12, and custom solar radiation force models known as T10 and T20 (Fliegel et al., 1992).

I<(ii'Ill *Models*

All three analysis systems use the IERS Standards set forth in IERS Tech Note 13 (McCarthy, 1993)('1'aJ~le.yet al.,this issue) for earth orientation and the deformation of the earth due to solid and pole tides. JPL's GPS solutions estimated polar motion and UT1 with nominal values taken from IERS Bulletin B finals or predicts, depending on the time of processing. The CSR and GSFC solutions employed polar motion and UT1 rate values determined by SLR data from Lageos (Tapley et al., this issue).

GIPSY-OASIS II Solution Scenario, Reduced Dynamic Processing

J]'], computed dynamic and reduced dynamic solutions with the GIPSY-OASIS 11 analysis software (Webb et al., 1993; Wu et a]., 1990). Its main components are a GPS data editor, orbit integrator, measurement model generator, and filter/snmother. The data editor operates on a combined set of dual frequency GPS phase and pseudorange measurements anti automatically detects outliers and carrier phase discontinuities (Blewitt, 1990). An automated executive tics the modules together producing daily orbit solutions unattended. The system typically produces a reduced dynamic solution within 2 days of onboard data acquisition, using less than 6 CPU hours on an }ll' 735 workstation.

The orbit integrator numerically integrates the satellite trajectory from a nominal initial state using precise models of the. forces acting on the satellite. 1(also computes partial derivatives of the current state of the spacecraft with respect to the dynamical and epoch state parameters. The trajectory and partials are the.n passed to the measurement model program,

After editing, the data are compressed to 5-rein normal points and the ionosphere-free combinations of phase and pseudorange are formed. In the compression step the pseudo-range data are smoothed against the carrier over the entire S-rein interval, while the phase is simply sampled at the appropriate times. Because the TOPEX/Poseidon onboard clock drifts freely with respect to the ground receiver clocks (which are kept close to UTC), we require a small interpolation of onboard phase to the appropriate. sample time to ensure common mode cancellation of SA dithering. This is accomplished with a cubic fit to four 1-sec points about the desired time (WU et al., 1992). The nominal trajectory is the.n used to compute model GPS observables and their partial derivatives with respect to all adjusted parameters. The measurement model program then retrieves the satellite positions and partials passed by the integrator, computes the model observables, and, in addition, partial derivatives of the observables with respect to ground station position, zenith troposphere delay, earth orientation, GPS clocks, and receiver clocks. The observable model includes relativistic effects, the Earth models discussed above, phase windup due to antenna rotation (Wu et al., 1993), anti antenna phase-mntcr variation as a function of azimuth and elevation (Zieger et al., 1994).

Next the filter/smoother takes over to carry out the grand solution for the TOPEX/Poseidon and GPS states, ground site positions (five are held fixed for reference), clocks, atmospheric delays, and so on. In its simplest mode, the filter/smoother produces the equivalent of a conventional batch least-squares solution; but to obtain a more accurate orbit, some parameters are treated as stochastic processes and adjusted at each time step in a time-sequential Square

Root Information Filter (SRIF) formulation (Bierman, 1977). The parameters adjusted in our standard solution strategy are summarized in Table 1.

in these solutions, all clocks are solved for freely and independently at each S-rein time step (i.e., modeled as while noise processes with no a priori constrain, except for one at a ground station which is held fixed as a reference clock. The zenith atmospheric delay at each ground site. is also adjusted at each step, modeled as a random walk which in 1 hr adds 1 cm uncertainty in the zenith delay. For the. 30-hour data arcs, the parameters of the T10 and T20 solar pressure model (Fliegel et al., 1992) are treated as loosely-constrained constants plus a small colored noise process with a 4-hour correlation lime and sigma of 10% at 1-hr batch times. The estimation of the GPS orbits is essentially dynamic.

The reduced dynamic solution is produced only in the final estimation step. First, the "TOPEX/Poseidon epoch state and the empirical constant and once- and twice-per-revolution accelerations (Eq. 3) are adjusted to convergence in a dynamic solution, which takes two passes through the filter. This dynamic solution is typically accurate to better than 20 cm (3D)), well within the linear regime for the final reduced dynamic adjustment. in the reduced dynamic step, adjustments are made to the TOPEX/Poseidon state and to all previously adjusted parameters except two types: the. empirical once- and twice-per-rev terms, which are now held fixed, and the constant accelerations ($\vec{C}$ in Eq. 3), which now become stochastic and are re-estimated at each time step to provide the local geometric corrections. The latter are modeled as first order Gauss-Markov (colored noise) processes and given a correlation time of 15 min with steady-state sigmas of 10, 20, and 20 nanometers/sec^2 in the radial, cross- and along-track directions. It is the. geometric strength of the GPS observations that allows these final stochastic adjustments to be made with high accuracy.

Tuning Stochastic Acceleration Parameters

The steady-state sigmas for the stochastic acceleration parameters were chosen through an empirical process in which solutions were generated with a range of sigmas, and the final values selected were those that minimized the RMS differences on the 6-hr orbit overlaps for several test arcs. Once chose.n they were held fixed in all processing. A better criterion might be altimeter crossover statistics, but those were. not available in our earliest processing and were late.r reserved as an independent test of orbit accuaracy (see tests below).

MSODP1, Gravity Tuning

The Center for Space Research/University of Texas at Austin used MSODP1 (Multi-satellite orbit cte.termination Program) for the GPS/Topex data processing. The program has been compared against UTOPIA, the sing,lc-satellite mbit determination program used for processing SLR and DORIS data, and the two have agreed at the centimeter level.

MSODP1 uses doubly differenced phase measurements between the. flight receiver and the ground stations at 30-sec intervals. For the experiments presented in this paper, no double differences between pairs of ground stations were used. All double differences were corrected for the ionosphere, and pseudorange measurements were used to compute each receiver clock offset from GPS time.

The MSODP1 uses a batch-least squares estimator implemented with a square-root-free. Givens algorithm for improved numerical stability. No apriori constraints are assigned to any estimated parameter. A simultaneous solution is performed for the TOPEX/Poseidon and all GPS satellite states, along with once/revolution parameters for TOPEX/Poseidon and radiation pressure parameters for the GPS satellites. A constant zenith tropospheric delay is estimate.d at each site every 2.5 hrs, and a phase bias parameter is estimated for each combination of TOPEX/Poseidon, GPS satellite and ground receiver. One-day solution arcs were used in all cases except for the tuning of the gravity field, where 3.3-day arcs were used.

SLR/DORIS Solutions

The precise orbit ephemeris (POE) produced for the alt i mete.r geophysical data records and released to the science community is computed dynamically by GSFC with SLR/DORIS data over 10 day arcs. They are released only after an extensive validation procedure (Tapley et al., this issue). We will make comparisons to these official orbits as a test of the GPS reduced dynamic mbits.

ORBIT QUALITY ASSESSMENT

First we describe internal consistency tests within the GIPSY-OASIS II processing system, and then compare the GPS reduced dynami c orbit S With the GSFC POE sol uti on s. Next we present altimetry crossover differences, which provide a test that is independent of all orbit determination techniques and software. Next we examine. the difference between the dynamic and reduced dynamic orbits prod uced with GIPSY-OASIS II to obtain inform ation on the geographically correlated orbit error and its spectral content. The CSR group has recently tuned the JGM-2 gravity model with GPS data; in the final test, dynamic solutions produced by CSR with the tuned field are compared to reduced dynamic solutions made with JGM-2.

Dynamic Internal Tests

Postfit Residuals

As pa of automated quality control, the software examines postfit phase and pseudo range residuals over he full arc Anomalous data points are automatically detected and removed. Phase residuals for the flight receiver are typically about 5 mm RMS; pseudorange residuals are typically 70 cm RMS. These values are oughly equal to the combined instrumental noise and multipath error expected on the two observables, implying no substantial mismodeling in the estimation process. The GPS data are in general of high quality; only 0.01% of data are detected as anomalous and removed from the filtered solution.

Orbit Overlap

TOPEX/Poseidon data are processed in 30-hr arcs centered on noon UTC (Fig. 6) This yields adjacent orbits with 6 hrs of overlap. Although the data in the overlap interval are common to the two arcs, he orbi solutions in the overlap are only partially correlated because of the largely ndependent determination of GPS dynamic orbits and ground station locations for each arc. The orbit overlap agreement is therefore a rough but somewhat optimistic indicator of orbit quality.

'o avoid the estimation edge effects (increased error at the ends of the solution arcs esulting from the absence of data on the other side to constrain he stochastic estimate) encountered with reduced dynamic solutions, 45-min segments from each end of the two solutions are omitted in the RMS comparisons. This corresponds to three imes the time used for the stochastic accelerations A sample of the orbit difference during the central 4.5 hours of the overlap is shown in Fig. 7. The RMS difference is 0.88 cm in altitude, 5.70 cm cross track and **3.44** cm along track. Fig. 8 shows the average RMS overlap agreement in altitude for all overlaps for twelve 1()-clay cycles. The agreement is consistently below 2 cm, with an average of about 1 cm. The anomalous value for cycle 21 appears to have been caused by data outages at Goldstone while Goldstone was used as the reference clock. We have since modified the automated analysis to prevent the use of a reference clock at a station with sizable outages. Cycle 19, which produced the best agreement, was the only cycle in which no GPS satellites passed through the earth's shadow. During such eclipses the GPS force and measure.mcnt model errors increase noticeably. The TOPEX/Poseidon dynamic overlap agreement (not shown) is consistently worse, giving single RMS altitude overlap differences as high as 5.6 cm anti an average RMS difference of about 2 cm.

External Tests

Comparison with NASA Precise Orbit Ephemeris (POE)

Figures 9 anti 10 show the RMS differences between J]'] .'s GPS solutions (both dynamic and reduced dynamic) and the NASA POE over six 1 0-day repeat cycles. The average RMS radial difference was 2.68 cm for the dynamic comparison and 3.33 cm for the reduced dynamic comparison. The maximum differences in radial position at any point over all six cycles were 12.2 cm (dynamic) anti 11.5 cm (reduced dynamic). We shall argue that the better RMS agreement between the two dynamic orbits is the result of common crews in JGM-2 and the non-gravitational force models, errors which are partially remove.d in the. reduced dynamic solution.

In comparing the JPL dynamic and reduced dynamic orbits against the NASA POE, a bias in the mean of the z coordinates of the Greenwich Reference Frame (pseudo-earth- fixed) of about 3 cm was noticed. This bias varies slightly from cycle to cycle and day to day (Tables

2, 3 and 4). Most of mean differences in the. x and y coordinates can be attributed to errors in JGM-2, as suggested by the much smaller differences in the dynamic solutions ('1'able 2) and the offset predicted by the JGM-2 covariance shown in Plate 1b (see discussion below on the geographical correlation of the radial errors). The mean z bias remains essentially unchanged whether a dynamic or reduced dynamic mbit is used in the POE comparison. The z bias also appears in comparisons of the. J]']. mbits to CSR orbits computed with either GPS or S1 .R/DORIS data (Table 8). We note that recent determinations of the geocenter from GPS ground data only have obtained decimeter level accuracy in the z component (Vigue et al., 1 992). inclusion of TOPEX/Poseidon data in geocenter solutions has improved the observability of this component to about the centimeter level (Tapley et al., 1993b; Malla et al., 1993). Although the observed z bias between the J]'] . and other orbits dots not appear to rc.fleet a limitation of GPS tracking, we have yet to identify its source and continue to look for it. A 3 cm translation in z reduces the RMS differences by about 3 mm.

If we assume that the errors in the reduced dynamic orbits and the 1'01 ;s, are uncorrelated wc can attempt to allocate the 3.33 cm RMS difference. An equal allocation would yield an RMS radial error of 2.35 cm for both solutions. 13c1ow, using altimeter crossover analysis and the geographical distribution of errors, we will argue that the errors between the two mbits arc largely uncorrelated and that the reduced dynamic orbit error is some.what smaller.

Altimeter Crossover Analysis

A key method for assessing the relative. radial accuracy of different orbits relies cm altimeter data collected by the spacecraft. TOPEX/Poseidon carries two nadir-pointing radar altimeters that measure the range to the sea surface with an uncertainty of less than 4 cm RMS (] 'u et al., Ibis issue). These range measurements can be used together with the precise radial orbit solution to determine the geocentric height of the sea surface. At the points in the ocean where the satellite ground tracks intersect on ascending and descending passes, two such determinations of sea height can be made. in the absence of errors in the radial component of the orbit and in the media corrections to the altimeter range, the height difference at the crossing point location is a measure of the true variability of the ocean surface.

Crossover observations from eight separate 1 0-day repeat cycles of the TOPEX/Poseidon ground track were used for this analysis (Aviso, 1993). Since there is a range bias of about 20 cm bet ween the two altimeter systems (Christensen et 211.; Menard et al., this issue), wc used only the data from the U .S. dual-frequency alti meter. All standard envi ronmental and sc:i-state corrections were applied and editing was performed based on the data flags provided with the crossover geophysical records. As crossovers may occur days apart, corrections for ocean dynamic effects, such as those attributable to tides (Cartwright and Ray, 1 990) and atmospheric pressure loading, were also applied. A confounding factor is the unmodeled sea height variation from changes in ocean currents and errors in tide models and media corrections. To mitigate the effects of current variations, we restricted our analysis to crossovers occurring within the individual cycles. Table 5 lists the global crossover statistics for the GPS reduced c1 ynamic orbits and for the two precise orbits provided with t he merged GDR products. Over 35,000 individual crossovers occurring in the period from January 30 to May 19, 1993 are represented in the global statistic,

The actual radial orbit error is difficult to quantify based on these statistics since the residuals also contain errors in the media corrections and unmodeled oceanographic effects. A large portion of the tidal and atmospheric pressure signal has been removed with global models, but a sizable signal remains. in order to address this difficulty, we have segregated a small number of crossovers from the original global data set using a highly restrictive. set of geophysical editing criteria (rl'able. 6). (No outlier editing was performed since it is impossible to guarantee they do not result from large excursions in the orbit error.) These editing criteria are designed to reduce the ocean variation component of the crossover residuals while maintaining a global distribution of data. To the extent that the geophysical and environmental corrections being interrogated are not correlated with the orbit error, this approach should help to better isolate the mbit error contribution.

Table 7 lists the global crossover statistics for the data remaining after the restrictive editing. Note that while only 3% of the original data remain, there are still over 1000 globally distributed observations (Fig. 11). The variance (energy) has been reduced by over 50%, corroborating that the scatter of the original data set primarily reflects contributions from non-orbit sources. Assuming that the residual variabilities are uncorrelated in a global sense on ascending and descending tracks, one could infer that the radial orbit error is less than 5 cm RMS ($7.03/\sqrt{2}$), regardless of the orbit solution under consideration. Contained in this figure is some residual error from the geophysical corrections and instrumental effects, as well as orbit error. On the other hand, if there are large stationary orbit errors that are highly correlated cm ascending and descending passes-. an extreme example is an error in the overall scale of the orbit- -then the crossover observations cannot observe them. Despite these caveats, the crossover statistics provide a powerful and independent tool for measuring orbit consistency and for gauging improvement. In this context, we note that the GPS-based reduced dynamic orbits yield the lowest crossover residuals. in particular, the variances of the crossover populat ions in both tables (cf. "Table. 5, 'Table 7) are about 10 cm^2 lower with the. reduced dynamic orbits, suggesting a consistent reduction in TOPEX/Poseidon orbit error. If we assume that 3-4 cm of error remains from residual errors in the environmental and geophysical corrections and from ocean variability (a purely speculative number), then we can estimate that the GPS reduced dynamic orbit has a radial RMS error of 2-3 cm while the various dynamic orbits have radial RMS errors of 3-4 cm.

Geographical Error Distribution

Past ocean altimetry missions have been plagued by what are known as geographically correlated orbit errors—that is, orbit solutions that are consistently biased in different geographic regions (Tapley and Rosborough, 1985). Such errors can confound the interpretation of altimetry data by mimicking large-scale features in the ocean topography from which circulation estimates are derived. Geographically correlated orbit errors are most commonly associated with errors in the gravity model, although coordinate system offsets and other factors may also play a role. A pre-launch covariance study by Rosborough and Mitchell (1990) showed that kinematic and reduced dynamic orbits, by reducing dependence on force models in general, could virtually eliminate the geographic correlation in the gravity-induced TOPEX/Poseidon orbit error at large-scales. We have corroborated this result using the actual GPS-based orbits for TOPEX/Poseidon.

The differences between GPS-based dynamic and reduced-dynamic TOPEX/Poseidon orbits over three 10-day periods beginning March 10, March 20, and April 1, 1993, respectively, have been analyzed in terms of the geographical distribution of errors (Christensen et al., 1993). This analysis suggests that the pre-launch gravity model, JGM-1 (Nerem et al., 1993), introduces geographically correlated errors having a strong meridional dependence. These errors can be approximated by a large-scale positive anomaly in the Indian Ocean and a large-scale negative anomaly in the eastern Pacific Ocean (Plate 1a). The global distribution and magnitude of these geographically correlated errors are consistent with pre-launch covariance analysis; moreover, the estimated and predicted global RMS error statistics are also in close agreement at 2.3 and 2.4 cm rms, respectively (Christensen et al., 1993).

The most compelling evidence that this anomaly is attributable to an error in the JGM-1 gravity model can be seen in Plate 1b, depicting the global distribution of the mean orbits] height differences between two GPS dynamic orbits produced with the. JGM-1 and JGM-2 gravity models. JGM-2 is basically the JGM-1 mode] tuned with TOPEX/Poseidon SLR and DORIS data gathered from September 20, 1992 through February 18, 1993 (Nerem et al., 1993). Note that these differences come entirely from the gravity model since this is the only difference between the two cases. This figure is remarkably similar to Plate la, with the exception that the meridional variation is smaller and there is less track iness, i.e. less disparity among neighboring tracks. It is important to note that no GPS data were used to obtain JGM-2, so it is impossible that a geographically correlated error in the GPS tracking system would appear as an alias in JGM-2.

Repeating the GPS analysis with the JGM-2 gravity model suggests that a portion of the meridional dependence observed in JGM-1 still remains (see Plate 1 c). Though JGM-2 is a clear improvement over JGM-1, a measurable amount, 1.2 cm rms, in the differences between reduced-dynamic and dynamic orbits determined with JGM-2 persists. The salient features in this figure have also been identified in comparisons between the GPS reduced dynamic orbit and the NASA POE (also based on JGM-2), though the interpretation of this result in the context of gravity error is complicated by evident coordinate system differences. (The apparent shift between the NASA POE anti the. GPS-based orbits along the spin axis is discussed elsewhere in this paper.) Fui the.r comparisons between various dynamic and reduced-dynamic orbits should help to separate anti identify the sources of the geographically correlated errors, Note that, as illustrated in Plate 1 b, classical dynamic orbit determination is also capable of observing small modeling, errors, such as those introduced by the pre-launch JGM-1 gravity model. To accomplish this, however, the force models must be tuned with comprehensive tracking data from many orbits.

It has long been recognized that differential GPS data can be used with dynamic orbit determination techniques to improve the earth's gravity mode] (Bertiger et al., 1992; Tapley et al., 1993). With an improved gravity model, GPS-based dynamic orbits will improve and, for TOPEX/Poseidon, should approach the accuracy of reduced-dynamic orbits. (Properly weighted, however, the reduced dynamic orbits will in theory remain superior, if only by a small amount, by reducing non-gravitational and residual gravity model errors.) For orbiters at much lower altitudes, gravity and aerodynamic forces are extremely difficult to model, and the reduced dynamic technique will be crucial if sub-decimeter accuracy is needed.

Spectrum Dynamic minus Reduced Dynamic Altitude

Figure 12 gives the amplitude spectrum of the dynamic-minus-reduced dynamic altitude over 10 days. The spectrum is typical of gravity model error in a dynamic solution, which, because of the daily rotation of the field, generates a suite of tones at 1/rev ± m/day (Rosborough, 1986). The ± m/day tones in the spectrum may also include artifacts from the daily orbit fits spliced together to form a 10-day solution. Notice that nearly all of the energy is at frequencies below twice/rev. Since we know of no forces that can cause significant high frequency satellite motion, the reduced dynamic process noise constraints (the time constant and steady-state sigmas) have been set to suppress high frequency corrections. Experiments have shown that when those constraints are relaxed and we go to a more fully kinematic solution, the high frequency components increase, but only slightly, and almost entirely as a result of tracking measurement noise rather than real satellite motion.

Gravity Tuning

A preliminary tuning of the JGM-1 prelaunch gravity model has been performed at CSR by augmenting the JGM-1 gravity coefficients and their associated covariance with new information equations from twenty 10-day repeat cycles of DORIS and SLR data, and four cycles of GPS data, from TOPEX/Poseidon. This field, referred to as TEG-3, is discussed in detail **in** Tapley et al. (1993). The SLR and DORIS tracking data were processed in 10-day arcs, while, for computational efficiency and to reduce GPS satellite dynamic error, the GPS data were processed in 3.3-day arcs. For both data sets, daily once/revolution empirical accelerations in the along track and **cross** track components, along with daily mean along track accelerations, were adjusted.

The RMS of the mean, or constant component of the geographically correlated gravity errors for TOPEX/Poseidon, predicted from the covariance, has been reduced from 1.6 cm for the JGM-2 model to less than 1 cm. The peak has been reduced from 2 cm ill JGM-2 to less than 1 cm in TEG-3. We attribute this to the additional geographic coverage provided by G1'S tracking, since an alternate field (TEG-3A), obtained with SLR and DORIS data only, yielded correlated errors approximately 50% larger. Separate gravity tuning solutions made with four cycles of GPS data only were gene.rally comparable to or better than those made with 20 cycles of SLR and DORIS data.

Dynamic orbits for TOPEX/Poseidon computed with TEG-3 using SLR/DORIS data give better agree.Jmcn(with the J}']. reduced dynamic orbits (Table 8) than the corresponding orbit using JGM-2. The radial RMS agreement is currently 2.5 cm over the nine cycles examined, after removing a z bias of 1.5 - 3.0 cm, with little spatially correlated signal. The three-dimensional RMS differences have also been improved for most cycles (Table 8). It should be recalled that nongravitational orbit errors are also included in these trajectory differences, although such errors are smallest in the radial component.

The geographically correlated portions of the differences between dynamic orbits computed with JGM-2 and TEG-3 are similar to those between JGM-2 dynamic and the J]'], reduced dynamic orbits, indicating that the reduced dynamic solution and the tuned gravity field solution have converged to a similar result, although they were arrived at through quite different filtering strategies. We regard this as evidence of both an improvement in the. gravity model and the efficacy of reduced dynamic filtering

REMAINING QUESTIONS

Topex/Poseidon GPS Antenna

Early in the GPS data analysis, a bias of ~6 cm in the radial direction was noted between reduced dynamic met dynamic orbits. Reduced dynamic tracking is sensitive to the position of the. phase center of the GPS receiving antenna, and the center of gravity (CG) of the satellite is inferred from attitude information and measurements of the antenna position made before launch. The dynamic solution, on the other hand, is highly sensitive to the satellite CG since that is the reference point for the orbital dynamics. By adding a radial bias parameter to the dynamic state estimate and fixing the result in the reduced dynamic estimate the bias between the reduced dynamic and dynamic orbits is eliminated. The formal error on the radial bias estimate is about 3.3 mm with 30 hrs of data. The mean of the radial bias estimate, determined with 30-hr arcs over more than 5 months from cycle 17 to cycle 33, is 59.9 mm, and its standard deviation is 4.S mm (Fig. 1 3). The maximum value occurs during a yaw ramp in the TOPEX/Poseidon attitude control, which might suggest a mismodeling of the yaw ramp. The minimum occurs during a planned TOPEX/Poseidon orbit maintenance maneuver. Figure 14 shows the time series during a period in which none of the GPS satellites are in eclipse. 'J'here arc known errors in the force model for the GPS spacecraft which are larger during eclipse. There are also known errors in the measurement model for GPS due to attitude mismodeling during eclipse. Both of these models can be improved. Note the smaller standard deviation of 1.6 mm during this period.

"1'here are two known systematic errors in the phase observable which when corrected change the antenna offset by 1.05 cm (leaving a total offset of about 5 cm) and affect the orbits by an RMS of 1-3 mm. Together (hey can be as large as 1.3 cm. The first is in the receiver decimation filler, which results from the signal's Doppler offset, and the second is in the Costas loop, which results from the Doppler rate. These phase. errors can be corrected with the following simple formula:

$$\Delta\rho = \frac{1}{2} T_c \dot{\rho} + \frac{1}{\omega_n{}^2} \ddot{\rho} \qquad [4]$$

where $\dot{\rho}$ and $\ddot{\rho}$ are the range rate ant] range acceleration corresponding to the Doppler ant] Doppler rate; $T_c = 0.976 \times 10^{-6}$ sec is the code correlation period; ω_n, the natural frequency of the Costas loop, is 29.3 radians/see for the 17 Hz loop noise bandwidth of the receiver.

The mechanical position of the antenna was measured in satellite coordinate to < 1 mm before launch. It agrees to the nominal location as specified on the drawings within 2 mm in the z component and within 8 mm 3D. An anomaly exists somewhere in the overall mode.1 of the GPS observable. Although an error in the satellite measurements would explain the results, wc have all but ruled that out based on other evidence and as yet have no satisfactory explanation for the apparent antenna bias. '1'here is a slim possibility that the offset could result from incomplete knowledge of the phase center of the GPS transmitters. A preliminary analysis, however, shows extremely small variation of the GPS satellite phase center with look angle. A Block-2 GPS transmit antenna from the qualification model satellite has been obtained from the USAF Space Command and is being calibrated at JPL. Meanwhile, wc continue to estimate a phase center offset, even though it is now well characterized.

IMPLICATIONS FOR THE FUTURE

Results from TOPEX/Poseidon show that pre-launch covariance studies were quite accurate and thus lend confidence to predictions made by similar studies for future missions. Figure 15 gives results from such a study performed several years before launch (Wu et al., 1991). The assumption (Table 9) were in many ways inconsistent with what has been done in the actual 30-hr GPS solutions. The available computing power at the time of the study was meager by today's standards, requiring the use of much shorter data arcs. To Compensate, we assumed a 2 m *a priori* error cm the GPS orbits and a low pseudorange noise of 5 cm, The estimated 2-3 cm RMS radial error for the reduced dynamic solution with JGM-2 is plotted (point x) in Fig. 15. in addition the typical RMS difference with SLR/DORIS solutions (with JGM-2) is plotted. Somewhat fortuitously, the artificial compensation has proved reasonably accurate, and the agreement with the. estimated actual error is within a centimeter.

An example of a possible future mission is taken from the Earth Observing System (EOS), a suite of scientific Earth probes planned to fly at about 700 km beginning in the late 1990's. Because dynamic model errors can grow large. at that altitude, a purely kinematic analysis is presented. This time the reference silt error is reduced to 3 cm per component and the number of flight receiver channels is increased to track all satellites in a hemisphere, which increases the geometric strength compared to TOPEX/Poseidon. Other assumptions that differ from the TOPEX/Poseidon covariance analysis are given in Table 10. Figure 16 shows the predicted altitude error as a function of data arc length for several different GPS data combinations. The data type called "carrier-quality range" is a fictitious pseudorange measurement having the precision of carrier phase, and serves to establish a performance bound. With data arcs longer than 20 hours, all scenarios yield about 2.5 cm RMS radial errors for kinematic tracking, which is completely independent of dynamic model error.

To see what might be done with even greater geometric strength we present a study of the Space Shuttle at 300 km in which we open up the flight receiver field of view to the full sky (each Shuttle is equipped with GPS antennas top and bottom to permit this). Typically, there will be 13-15 GPS satellites in view at once. Other assumptions are given in Table 1] . As shown in Fig. 17, the limiting error in all components now falls below **2 cm.** This **opens** up new possibilities for near-earth ocean altimetry, and for short-duration testing of precise instruments on the Shuttle.. We should note, however, that covariance analysis can be optimistic, particularly for kinematic estimation, and unmodeled systematic errors could at least double the actual error in these examples.

CONCLUSIONS

The evidence suggests that we are obtaining a radial orbit accuracy for TOPEX/Poseidon of better than 3 cm RMS with the GPS reduced dynamic technique. Tests of orbit quality include postfit phase residuals (-5 mm), orbit overlap comparisons (~1 cm radial RMS), comparison with GSFC POEs (3.3 cm radial RMS; 11.5 cm maximum difference for 6 cycles), and altimeter crossovers (10 cm^2 smaller variance than GSFC POE or CNES orbits). The reduced dynamic orbits are seen to reduce significantly the geographically correlated error arising from the gravity model. Tuning of the gravity model with GPS data has resulted in a similar reduction of geographically correlated error in subsequent dynamic orbit solutions with all data types. Future missions can take advantage of the low cost operational GPS system developed for the TOPEX/Poseidon experiment and should obtain radial RMS accuracies of 5 cm or better in orbits as low as a few hundred kilometers.

ACKNOWLEDGMENT

The work described in this paper was carried out in part by the Jet Propulsion Laboratory, California Institute of Technology, under contract with the National Aeronautics and Space Administration. We thank Steve Nerem of Goddard Space Flight Center, John Ries of the Center for Space Research at University of Texas, and George Rosborough of the. University of Colorado for their help and comments. The GPS Network operations Group at JPL provided automated access to the data from the GPS ground network (sponsored by NASA's Office of Space Communications). The work of the POD Team headed by Byron Tapley from GSFC, CCAR, CSR provided valuable information on modeling TOPEX/Poseidon, kept us all honest, and provided a healthy impetus to work hard. The computer systems and network support of Mike Urban and Michael Kelsay contributed to the JPL systems case of USC. The Satellite Geodesy and Geodynamics Systems Group at JPL is jointly responsible for the GIPSY-OASIS II and made many valuable contributions to this work.

REFERENCES

Bertiger, Willy I., J. T. Wu, and Sien C. Wu, Gravity Field Improvement Using GPS Data From Topex/Poseidon: A Covariance Analysis, Journal of Geophysical Research, Vol. 97, 112, pgs. 1965-1971, Feb. 10, 1992.

Bierman, G. J., *Factorization Methods for Discrete Sequential Estimation*, Academic Press, Orlando, FL., 1977.

Blewitt, G., An automatic editing algorithm for GPS data, *Geophys. Res. Lett., 17*(3), 199-202, 1990.

Blewitt, G., M. B. Heflin, K.J. Hurst, D.C. Jefferson, F.H. Webb and J.F. Zumberge, Absolute far-field displacements from the 28 June 1992 Landers earthquake sequence, *Nature, 361*, 340-342.1993.

1]01"11, G., M. Parke, J. Johnson, 'I'. Kelecy, C. Rocken and E. Christensen, TOPEX altimeter height calibration using a GPS buoy, submitted to *JGR* TOPEX/Poseidon Special Issue, Nov 1993.

Christensen, E. J., B.J. Haines, K.C. McColl and 1{. S. Nerem, Observations of geographically correlated orbit errors for TOPEX/Poseidon using the Global Positioning System, *Geophys. Res. Lett.*, 1994 (to appear).

Christensen, E. J., C. S. Morris, B. J. Williams, J. R. Guinn, B. J. Haines, C. K. McColl, R. A. Norman, S. J. Keihm, D. A. Imel and G. H. Born, Calibration of TOPEX/Poseidon at platform harvest, submitted to *JGR* TOPEX/Poseidon Special Issue, Nov 1993.

Fliegel, 11. 1'., T. E. Gallini and E. R. Swift, Global Positioning, System radiation force models for geodetic applications, *J. Geophys. Res., 97*(B1), pp 559-568, 1992.

Fu, L. L., and M. Lefebvre, TOPEX/Poseidon mission overview, submitted to *JGR* TOPEX/Poseidon Special Issue, Nov 1993.

Kaplan, M. 11., *Modern Spacecraft Dynamics and Control,* John Wiley and Sons, 1976.

Lerch, F., R Nerem, J. Marshall, B. Putney, E. Pavlis, S. Klosko, S. Luthcke, G. Patel, N. Pavlis, R Williamson, J. Chan, B. Tapley, C. Shum, J. Ries, R. Eanes, M. Watkins anti B.

Schutz, Gravity model improvement for TOPEX/Poseidon, *EOS Trans. AGU, 74*(16), p. 96, Apr 1993.

Malla R. P., S. C. Wu, S. M. Lichten and Y. Vigue, Breaking the ΔZ barrier in geocenter estimation, *Eos, Trans. AGU, 74(43)*, 182, 26 Ott 1993.

Marshall, J. A., S. B. Luthcke, P. G. Antreasian and G. W. Rosborough, Modeling radiation forces acting on TOPEX/Poseidon for precision obit determination, NASA Technical Memorandum 104564, Jun 1992.

McCarthy, D. D. (ed.), *IERS Technical Note 13*, Central Bureau of IERS - Observatoire de Paris, Jul, 1992.

Melbourne, W. G., E. S. Davis, B. D. Tapley and T. P. Yunck, The GPS flight experiment on TOPEX/Poseidon, *Geophys. Res. Lett.*, 1994 (to appear).

Milliken, R. J. and C. J. Zoller, Principle of operation of NAVSTAR and system characteristics, *Navigation*, 2.5, 95-106, 1978.

Neilan, R. E. and C. E. Nell, The IGS core and fiducial networks: current status and future plans, Proc. 1993 IGS Workshop, Astronomical Institute, Univ. of Bern, Mar 1993.

Nerem, R. S., F. J. Lerch, J. A. Marshall, E. C. Pavlis, B. H. Putney, J. C. Chan, S. M. Klosko, S. B. Luthcke, G. B. Patel, N. K. Pavlis, R. G. Williamson, B. D. Tapley, R. J. Eanes, J. C. Ries, B. E. Schutz, C. K. Shum, M. M. Watkins, R. H. Rapp, R. Biancale and F. Nouel, Gravity model development for TOPEX/Poseidon: Joint Gravity Model 1 and 2, submitted to *JGR* TOPEX/Poseidon Special Issue, Nov 1993.

Rim, 11., TOPEX orbit determination using GPS tracking system, Ph.D. dissertation, The University of Texas at Austin, Austin 'l'X, Dcc 1992.

Rosborough, G. and S. Mitchell, Geographically correlated orbit error for the Topex satellite using GPS tracking, AlAA 90-2956, Pmt. AIAA/AAS Astrodynamics Conf., Part 2, Portland, OR, 655-663, Aug 1990.

Rosborough, G. W., *Satellite orbit perturbations due to the geopotential, Ph.]).* thesis, 155 pp., Univ. of Tex., Austin, Jan 1986.

Schutz, B. ii., B. D. Tapley, P. A. M. Abusali and H. J. Rim, Dynamic orbit determination using GPS measurements from TOPEX/Poseidon, *Geophys. Res. Lett.*, 1994 (to appear) .

Spilker, J. J., GPS signal structure and performance characteristics, *Navigation, 2.5, 29-54,* 1978.

Tapley, *13.*, J. C. Ries, G. W. Davis, R. J. Eanes, C. K. Shum, M. M. Watkins, J. A. Marshall, R. S. Nerem, 11.11. Putney, S. M. Klosko, S. B. Luthcke, D. Pavlis, R. G. Williamson, and N. P. Zelensky, Precision orbit determination for TOPEX/Poseidon, submitted to *JGR* TOPEX/Poseidon Special Issue, Nov 1993a.

Tapley, B. D., M. M. Watkins, J. C. Ries, G. W. Davis, R. J. Eanes, S. R. Poole, H. J. Rim, B. E. Schutz, and C. K. Shum, 'l'he. TEG-3 Gravity Model, to be submitted to Journal of Geophysical Research, 1993b.

Vigue, Y., G. Blewitt, S. M. Lichten, M. B. Heflin, and R. J. Muellerschoen, Recent High-Accuracy GPS Estimates of the Geocenter, EOS Transactions, American Geophysical Union, Vol. 73, No. 43, pg. 135, October 1992.

Watkins, M. M., J. C. Ries and G. W. Davis, Absolute positioning using DORIS tracking of the SPOT-2 spacecraft, *Gepohys. Rev. Lett.*, 19(20), 2039-2042, 1992.

Webb, F. H and J. F. Zumberge, eds., *An Introduction to GIPSY/OASIS II*, JPL Course Notes, Boulder Colorado, Jul 1993.

Wu, J. T., S. C. Wu, G. H. Hajj and W. I. Bertiger, Effects of antenna orientation on GPS carrier phase, *Manuscript Geodetica, 18*(2), *pp. 91-98,* 1993.

Wu, S. C. and V. J. Ondrasik, Orbit determination of low-altitude Earth satellites using GPS RF Doppler, *Proc. IEEE Position Location and Navigation Symp.*, Atlantic City, NJ, 85-91, Dec 1982.

Wu, S. C., T. P. Yunck and C. L. Thornton, Reduced-dynamic technique for precise orbit determination of low earth satellites, paper AAS 87-410, AAS/AIAA Astrodynamics Specialist Conf., Kalispell, Montana, Aug 1987, Also apears in *J. Guid., Control and Dynamics, 14(1),* pp. 24-30, Jan-Feb 1991.

Wu, S. C., Y. Bar-Sever, S. Bassiri, W. I. Bertiger, G. A. Hajj, S. M. Lichten, R. P. Malla, B. K. Trinkle and J. T. Wu, *Topex/Poseidon Project: Global Positioning System (GPS) Precision Orbit Determination (POD) Software Design*, JPL D-7275, Mar 1990.

Wu, S. C., W. 1. Bertiger and J. '1', Wu, Minimizing selective availability error on Topex GPS measurements, *J. Guidance, Control and Dynamics, 1.5(5), pp. 1306-1309,* Sept- Oct 1992.

Yunck, T. P. and Wu, S. C., Non-dynamic decimeter tracking of Earth satellites using the Global Positioning System, AIAA paper 86-0404, AIAA 24th Aerospace Sciences Meeting, Reno, NV, Jan 1986.

Yunck, T. P., W. 1. Bertiger, S. C. Wu, Y. Bar-Sever, E. J. Christensen, B. J. Haines, S. M. Lichten, R. J. Muellerschoen, Y. Vigue and P. Willis, First assessment of G}'S-based reduced dynamic mbit determination on TOPEX/Poseidon, *Geophys. Res. Lett.*, 1994 (to appear).

Zierger, A. R., G. C. Cleven, E. S. Davis, F. S. Soltis, and C. 1.. Purdy, Sate.llitc/sensors for monitoring Earth's oceans from space, *Marine Geodesy, Special Issue*, Spring 1994 (to appear).

TABLES

Table 1. Estimation Scenario for Dynamic Filtering

of Topex/Poseidon orbit, GIPSY-OASIS II

Data Type	Data Weight
Ground Carrier Phase	1 cm
Ground Pseudorange	1 m
T/P Carrier Phase	2 cm
T/P Pseudorange	3 m

(all parameters are treated as constants unless otherwise specified)

Estimated Parameters	Parameterization	a priori constraint
T/P Epoch State	3-D epoch position	1 km
	3-D epoch velocity	10 cm/s
T/P Empirical forces	constant	1 1)1111/s2
(cross track & along track)	1- & 2-cycle-per-rev	1 mm/s^2
T/P Antenna Phase Center offset	radial	5 m
GPS States	3-D epoch position	1 km
	3-D epoch velocity	1 cm/s
GPS Solar Radiation Pressure	Coil.vfatll:	
	solar pressure scale factor	100 %
	Y-bias	$2x10^{-3}$ µm/s^2
	process-noise:	1 hrs batch; 4 hrs correlation
	X and Z scaling factor	10 %
	Y-bias	10^{-4} µm/s^2
Non-Fiducial Station Location	ECEF rectangular coordinates	1 km
Tropospheric delay	random-walk zenith delay	50 cm; o.17 111113/s $^{1/2}$
Pole Position	X and Y pole	5 m
Pole Position Rate	X and Y pole rate	1 m/day
UT1-UTC Rate	constant	100 s/day
Carrier Phase Biases	constant over a continuous pass	$3x10^5$ km
GPS and Receiver Clocks	white-noise	1 sec

Table 2. Mean Coordinate Difference, GSFC POE — Dynamic

Cycle	X (cm)	Y (cm)	Z (cm)
18	0.059	0.75	2.96
24	0.488	0.11	1.75
25	1.06	0.604	2.66
30	0.211	0.00452	3.75
31	0.183	-0.0398	3.59
32	0.355	-0.134	1.78

'J'able 3. Mean Coordinate Difference, GSFC POE — Reduced Dynamic

Cycle	X (cm)	Y (cm)	Z (cm)
18	1.23	1.24	2,91
24	2.72	0.721	1.44
25	2.24	0.311	2.24
30	1.7	0.387	3.28
31	1.49	0.494	3.27
32	1.63	1.1	2.21

Table 4 Daily Mean Difference in Z Coordinates, Cycle 18

	Goddard/JPL dynamic Z(cm)	Goddard/JPL reduced dynamic Z(cm)
93mar10	3.06	3.51
93mar11	4.45	4.06
93mar12	3.56	2.93
93mar13	2.43	2.28
93mar14	2.50	2,00
f)31nal'15	0.98	0.82
93mar16	5.57	439
93mar17	1.31	2.33
avera_e	2.98	2.86

'1'able S. Altimeter Crossover Statistics

Orbit	No.	Mean (cm)	RMS (cm)	Var (cm^2)
GPS **Reduced** Dynamic	36403	-0.04	9.69	93.84
NASA Precise Ephemeris	36403	0.35	10.22	104.41
CNES Precise Ephemeris	36403	1.04	10.13	101.47

Table 6. Restrictive Editing Criteria for Crossover Evaluation

PARAMETER	EDIT CRITERIA	REFERENCE
Sea state	Significant wave height < 1 m 01> 4m.	Aviso [1993]
Ocean tides	Difference of fide models >5 cm.	Cartwright and Ray (1990), Schwidcrski (1980)
Pressure loading	Inverted barometer> 10 cm	Aviso (1993)
Wind speed	Wind speed > 10 m/s	Aviso (1993)
Sea level variability	Mesoscale variability > 12 cm (RMS)	Koblinsky ct al. (1991)
Height interpltn.	Cubic spline fit RMS > 5 cm	Aviso (1993)

Table 7. Altimeter Crossover Statistics for Restrictive Editing Approach

Orbit	No.	Mean (cm)	RMS (cm)	Var (cm^2)
GPS Reduced Dynamic	1233	0.32	6.16	37.85
NASA Precise Ephemeris	1233	0.68	6.86	46.56
CNES Precise Ephemeris	1233	1.92	7.03	45.68

A

Table 8. SLR/DORIS UTOPIA orbit comparisons with JPL **reduced** dynamic **trajectories**

Cycle	JGM-2 Radial RMS	JGM-2 3D RMS	TEG-3 Radial RMS	TEG-3 3D RMS	Z Shift
14	3.2	13.9	2.4	12.5	1.6
15*	3.3	12.4	2.5	12.1	2.6
17*	3.2	13.2	2.9	14.4	2.3
18	2.9	12.9	2.6	11.8	2.3
19*	3.1	13.7	2.8	14.8	3.2
20	3.2	13.5	2.6	13.1	3.0
21	2.9	11.7	2.3	12.0	2.2
32	2.8	14.2	2.4	13.3	2.2

All units cm. * indicates GPS tracking from this cycle used in gravity solution.

TABLE 9. Error Model for Topex/Poseidon Orbit Determination Analysis

System Characteristics

Orbit (circular):	1334 km, 66° inclination
Number of Ground Site.s:	6 (including 3 fiducial sites)
Number of GPS Satellites:	18
Flight Antenna Field of View:	Hemispherical
Flight Receiver Tracking Capacity:	6 Channels (L1 & L2)
Data Types:	L1 & L2 pseudorange L1 & L2 carrier phase
Data into val:	5 Minutes
Smoothed Data Noise:	5 cm pseudorange 1 cm carrier phase

Adjusted Parameters & A Priori Errors

Topex/Poseidon Epoch State:	1 km; 1 m/sec, each component
GPS Satellite Stales:	2 m; 0.2 mm/sec, each component
Carrier Phase Biases:	10 km
GPS & Receiver Clock Biases:	3 msec (modeled as white noise)
Non-Fiducial Ground Locations:	20 cm each component

Fixed Errors Evaluated

Fiducial Site Positions:	5 cm each component
GM of Earth Uncertainty:	1 part in 10^8
Earth Gravity Error Model:	0- 100% GEM 10-GEML2 (20x20)"
Zenith Atmospheric Delay Error:	1 cm (modeled as random walk)
Atmospheric Drag Error:	10% of Total
Solar Radiation Pressure Error:	10% of Total

TABLE 10. Changes from Table 9 for Earth Observing System Kinematic Orbit Determination Analysis

Orbit (circular):	705 km, 98° inclination
Number of GPS Satellites:	24
Flight Receiver Tracking, Capacity:	All in View (within hemisphere)
Zenith Atmospheric Delay Error:	Adjusted as Random Walk
Fiducial Location Error:	3 cm each component
Earth Gravity Error Model:	100% GEM10-GEML2 (20x20)"

TABLE Changes from Table 9 for Shuttle
Kinematic Orbit Determination Analysis

Orbit (circular):	300 km, 28° inclination
Number of GPS Satellites:	24
Number of Ground Sites:	11 (including 3 fiducial sites)
Flight Antenna Field of View:	Full Sky
Flight Receiver Tracking Capacity:	All in View
Smoothed Data Noise:	5 cm pseudorange
	5 mm carrier phase
Zenith Atmospheric Delay Error	Adjusted as Random Walk
Fiducial Location Error	1.5 cm each component
Earth Gravity Error Model:	50% GEM [illegible] 2 (20x20)

FIGURE CAPTIONS

1 'ig. 1 Reduced Dynamic Tracking

Fig. 2 GPS tracking system for TOPEX POD.

1 'ig. 3. GPS Constellation with TOPEX.

] 'ig. 4 TOPEX/Poseidon Satellite

Fig. 5 GPS Global Tracking Network

Fig. 6. Overlapping data arcs and orbit solutions

Fig. 7. Comparison of overlapping TOPEX/Poseidon reduced dynamic orbit solutions '

Fig. 8. TOPEX/Poseic1on radial reduced dynamic orbit overlaps for twelve complete 10-day cycles

Fig. 9. Comparison of TOPEX/Poseidon dynamic orbit solutions with GPS against Goddard Space Flight Center S1 .R/DORIS orbits

Fig. 10. Comparison of TOPEX/Poseidon reduced dynamic orbit solutions with GPS against Goddard Space 1 'light Center S1 .R/DORIS orbits

Fig. 11 Global distribution of altimeter crossovers used to evaluate orbit accuracy. A stringent editing strategy (Table 6) was applied to crossovers formed from altimeter observations between January 30 and May 19, 1993.

Fig. 12. Radial amplitude spectrum dynamic minus reduced dynamic

Fig. 13 Body Fixed Z antenna offset, daily solution

Fig. 14 Body Fixed Z antenna offset, daily solution during a rare period of time in which no GPS arc. in eclipse

Fig. 15. Prelaunch Covariance Studies for TOPEX/Poseidon with 2 and 6-hr data arc lengths for a range of gravity errors. Actual RMS differences between Dynamic and Reduced Dynamic Solutions for 30-hr arcs are shown with point a. Point x marks an estimate of the radial error in 30-hr reduced dynamic solutions.

Fig. 16. Covariance analysis prediction for future a 700 km altitude mission.

Fig. 17 Predicted error for the Space Shuttle viewing all possible GPS within a sphere

Plate 1. (a) Geographic representation of orbit height differences for GPS-based dynamic and reduced-dynamic orbits using the JGM-1 gravity model. A 10 X 10 spherical harmonic fit to the data captures a signal with rms amplitude of 2.3 cm.

Plate 1. (b) Geographic representation of orbit height differences for JGM-1 and JGM-2 GPS-based dynamic orbits.

Plate 1. (c) Geographic representation of orbit height differences for GPS-based dynamic and reduced-dynamic orbits using the tuned JGM-2 gravity model. A 10 X 10 spherical harmonic fit to the data captures a signal with rms amplitude of 1.2 cm.

FIGURES

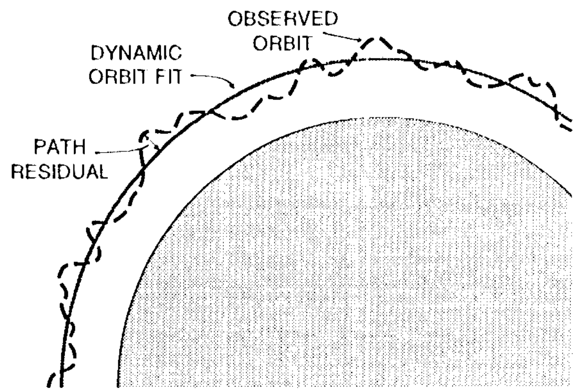

Fig. 1. Reduced Dynamic Tracking

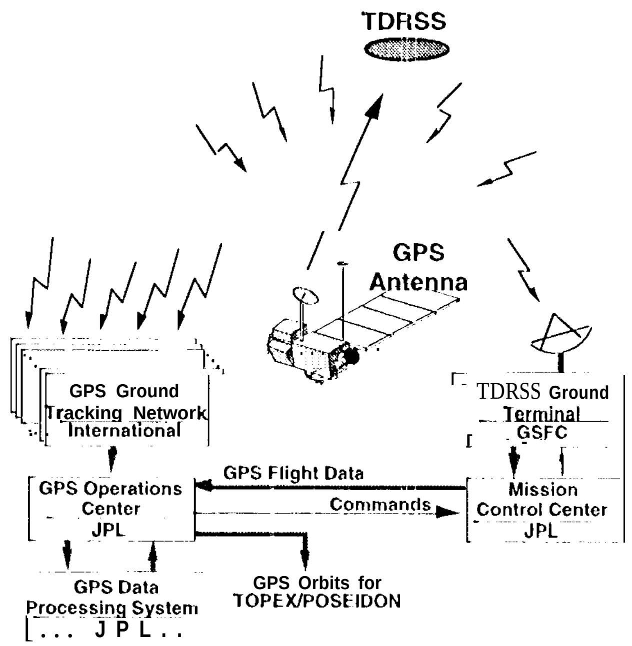

Fig. 2. GPS tracking system for TOPEX POD.

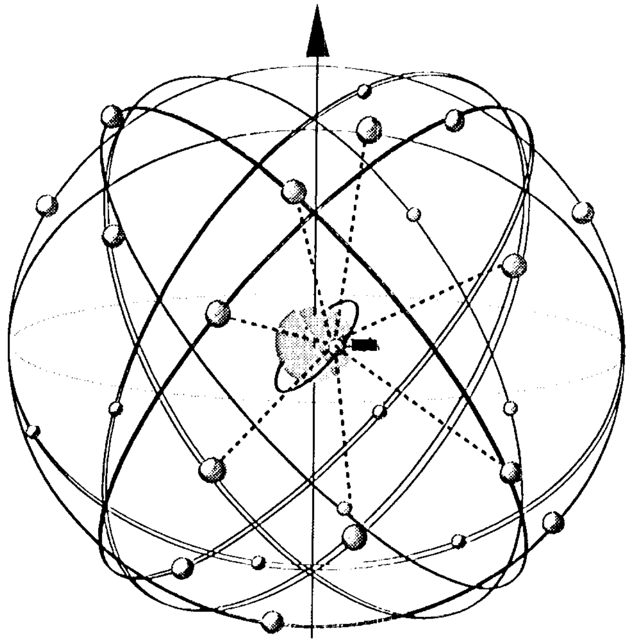

Fig. 3. GPS Constellation with TOPEX.

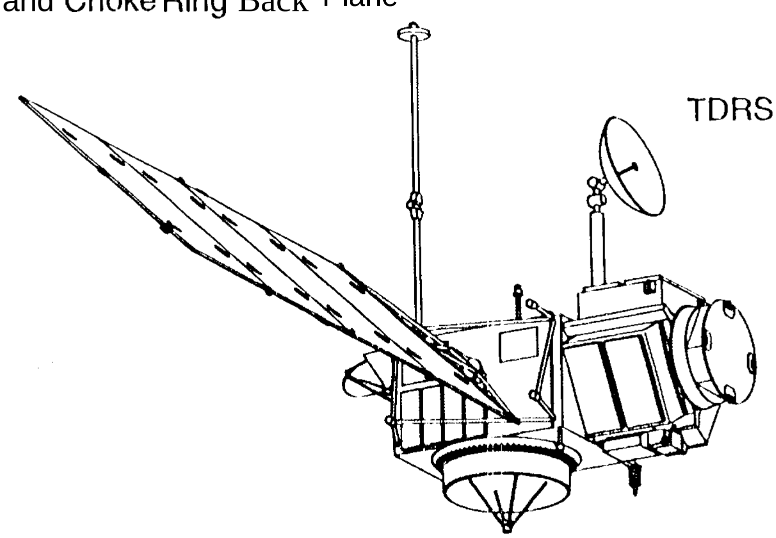

Fig. 4 TOPEX/Poseidon Satellite

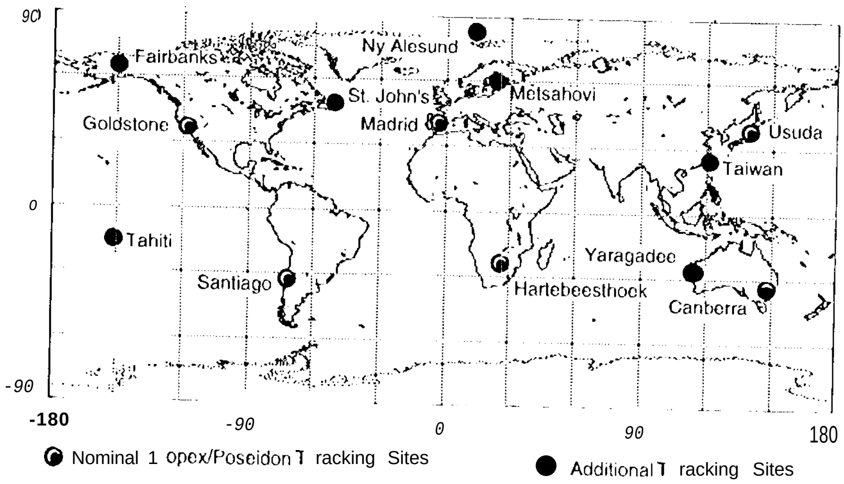

Fig. S. GPS Global Tracking Net work

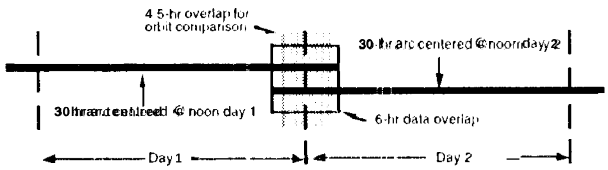

Fig. 6. Overlapping data arcs and orbit solutions

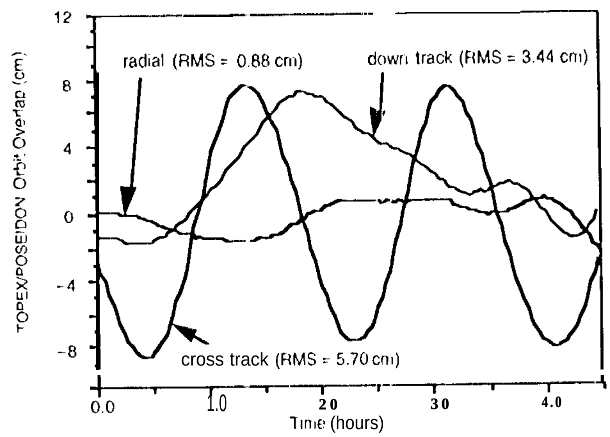

Fig. 7. Comparison of overlapping TOPEX/Poseidon reduced dynamic orbit solutions

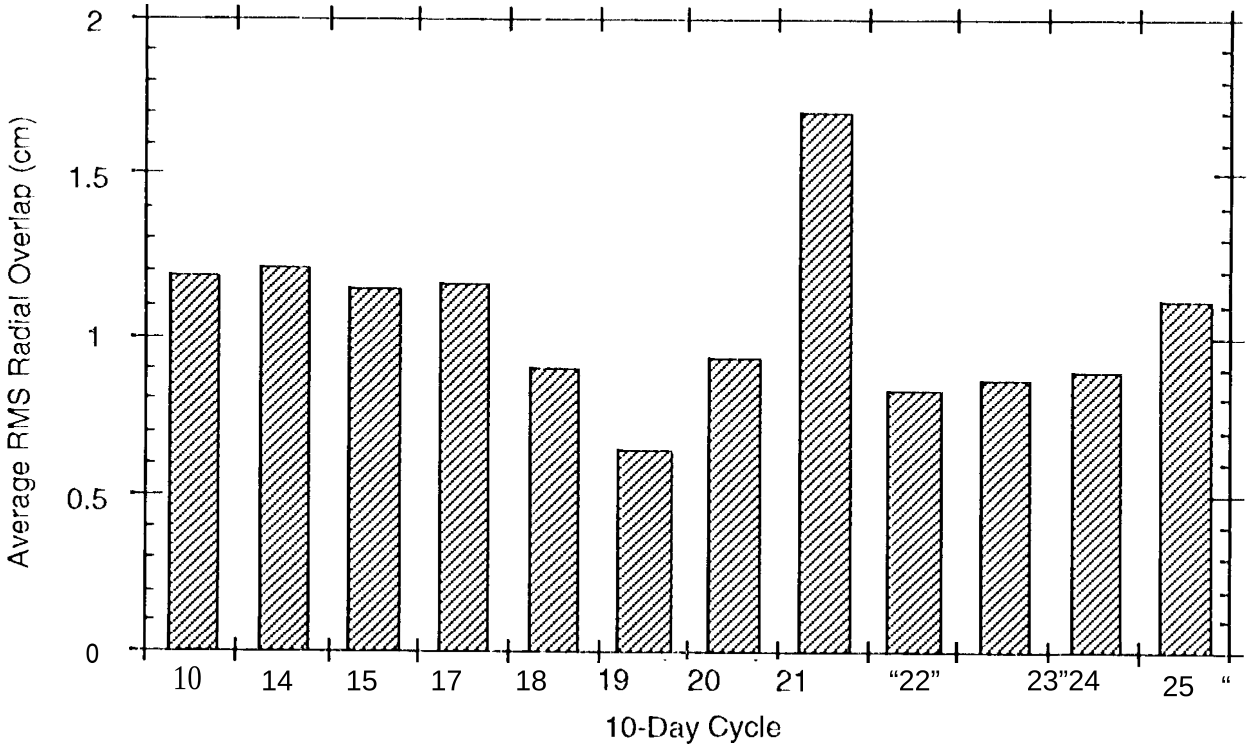

Fig. 8. TOPEX/Poseidon radial reduced dynamic orbit overlaps for twelve complete 10-day cycles

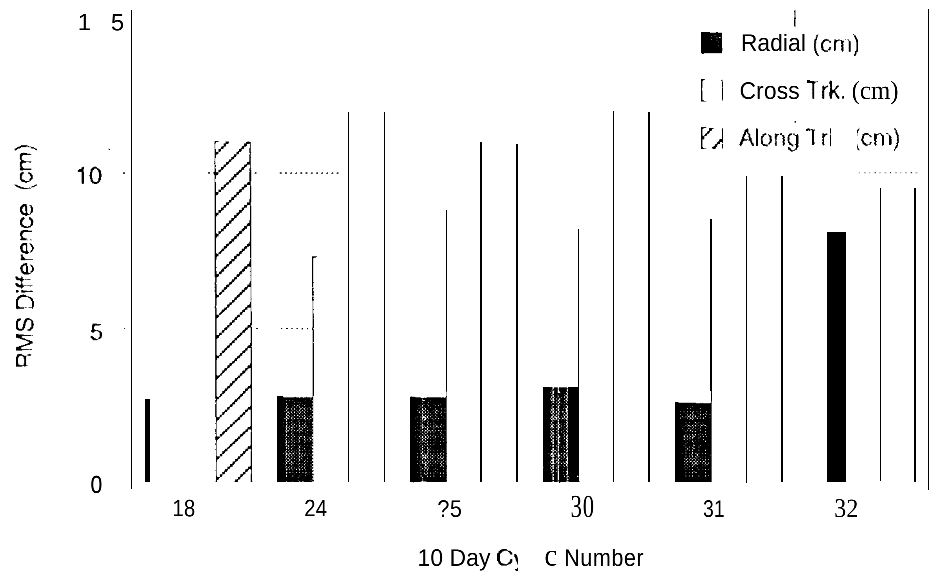

Fig. 9. Comparison of TOPEX/Poseidon dynamic orbit solutions with GPS against Goddard Space Flight Center SLR/DORIS orbits

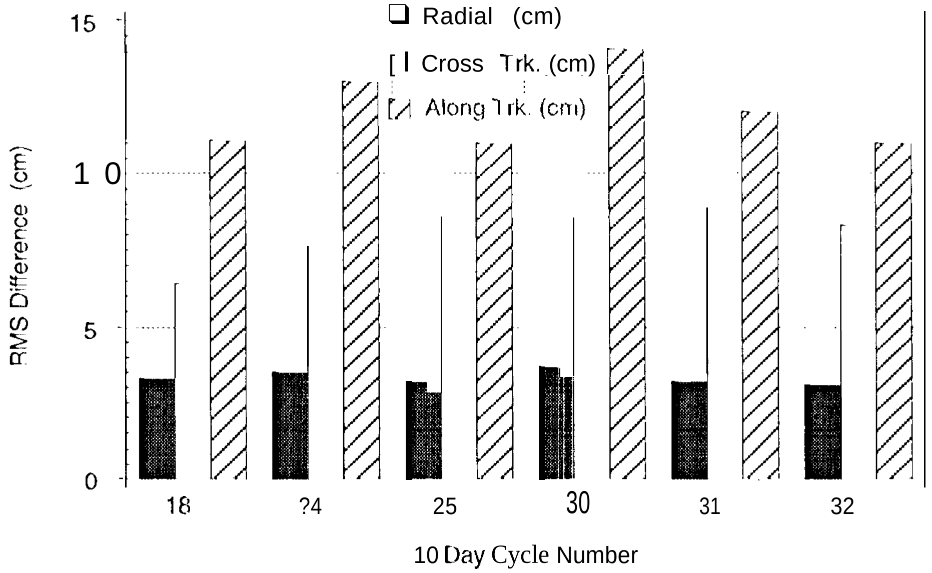

Fig. 10. Comparison of TOPEX/Poseidon reduced dynamic orbit solutions with GPS against Goddard Space Flight Center SLR/DORIS orbits

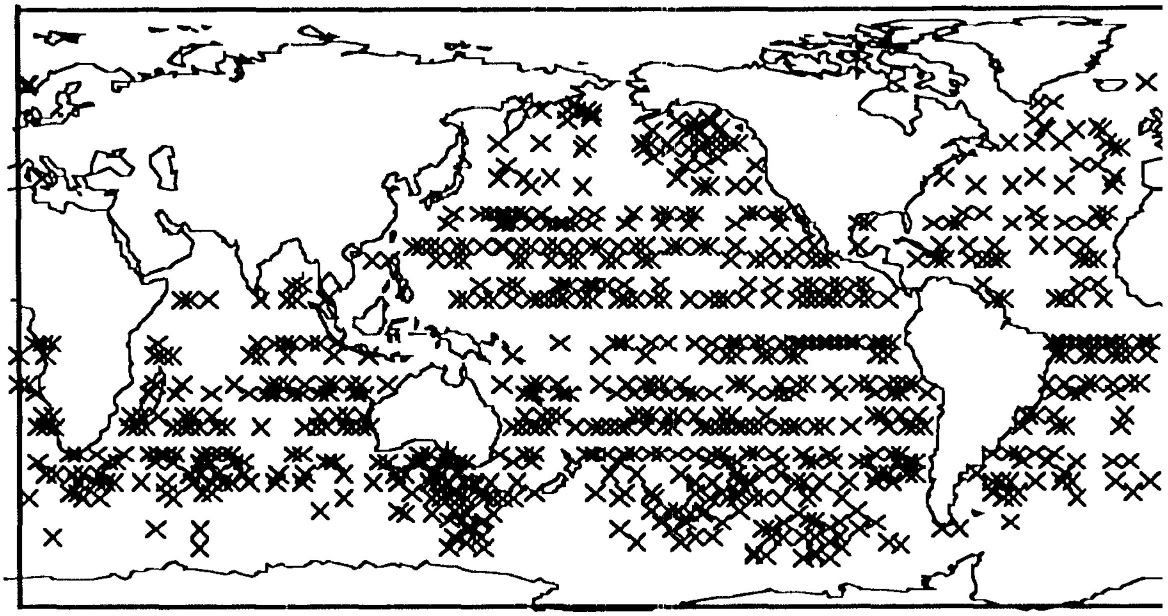

Fig. 11. Global distribution of altimeter crossovers used to evaluate orbit accuracy. A stringent editing strategy (Table 6) was applied to crossovers formed from all imeter observations bet ween January 30 and May 19, 1993.

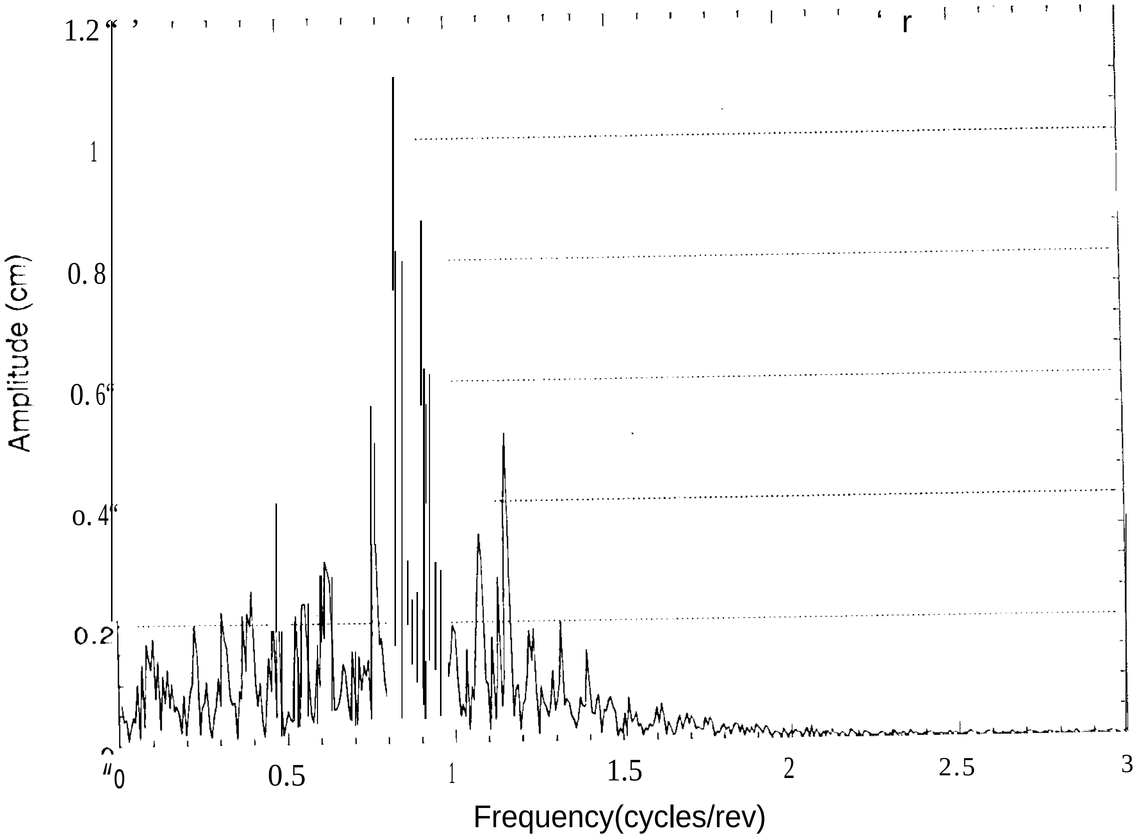

Fig. 12. Radial amplitude spectrum dynamic minus reduced dynamic

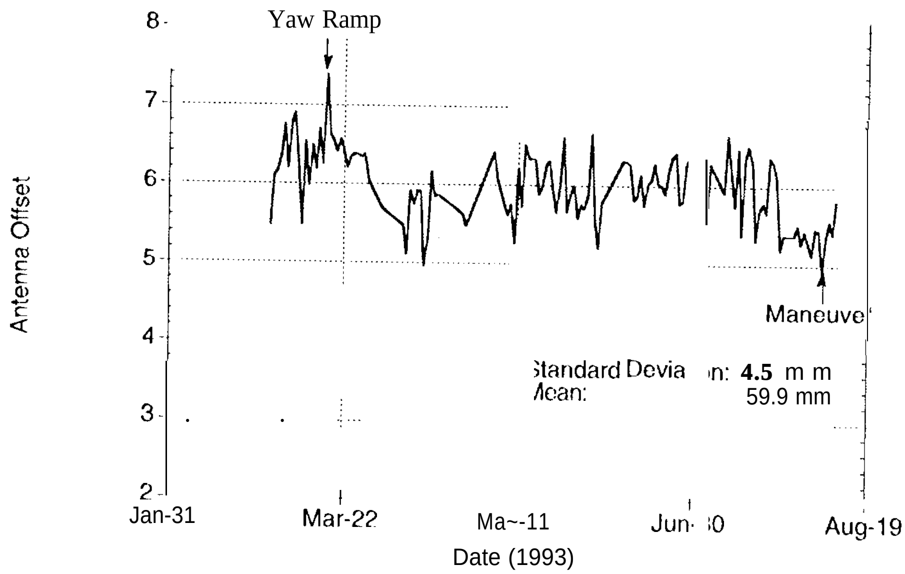

Fig. 13 Body Fixed Z antenna offset, daily solution

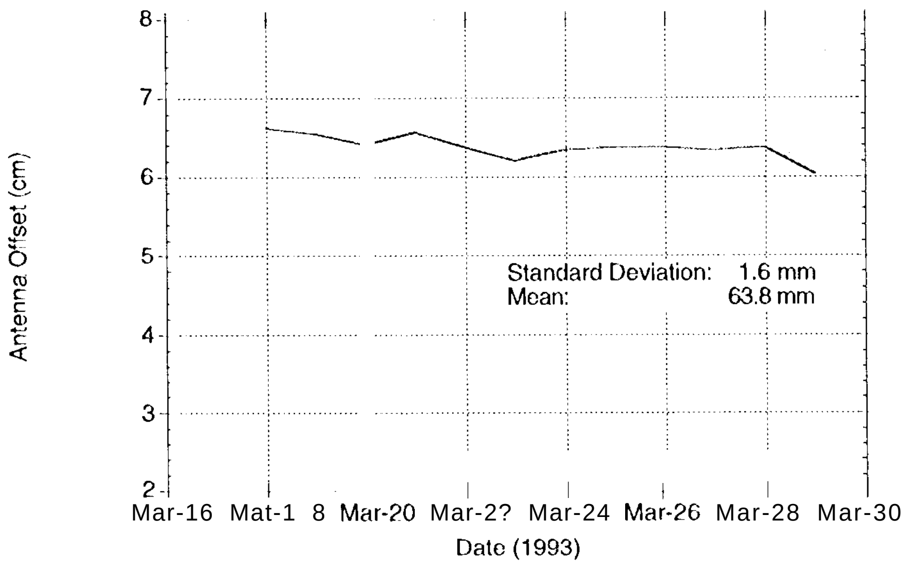

Fig. 14 Body Fixed Z antenna offset, daily solution during a rare period of time in which no GPS are in eclipse

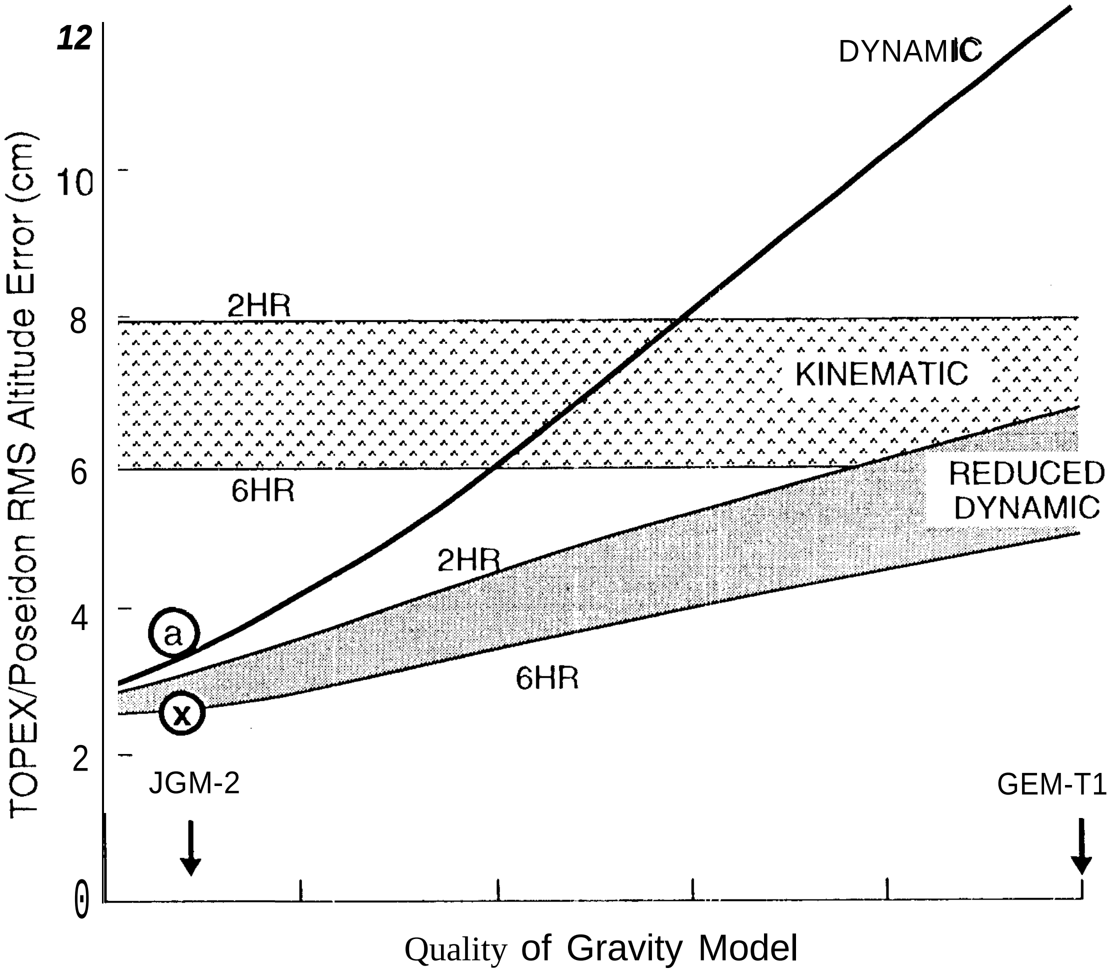

Fig. 15. Prelaunch Covariance Studies for topex/poseidon with 2 and 6-hr data arc lengths for a range of gravity errors. Actual RMS differences between Dynamic and Reduced Dynamic Solutions for 30-hr arcs are shown with point a. Point x marks an estimate of the radial error in 30-hr reduced dynamic solutions.

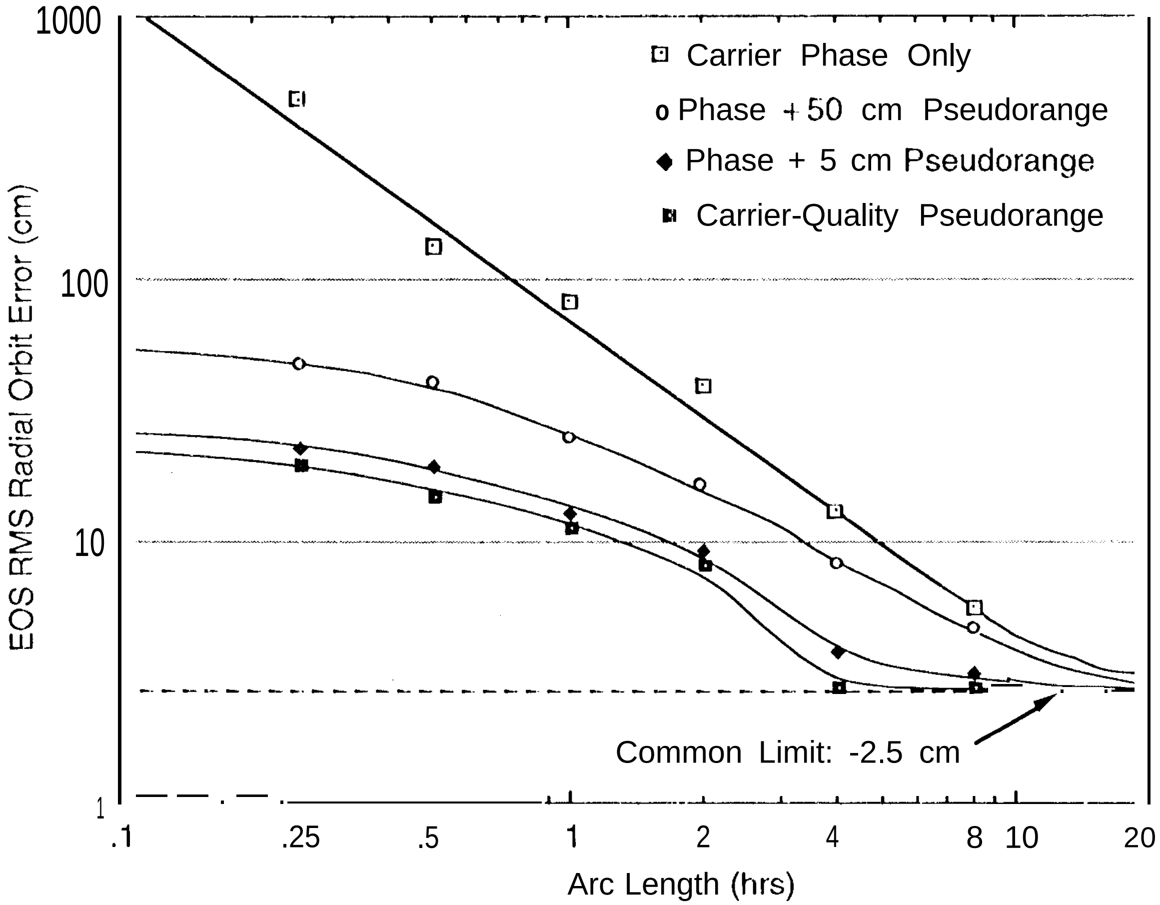

Fig. 16. Covariance analysis prediction for future a 700 km altitude mission.

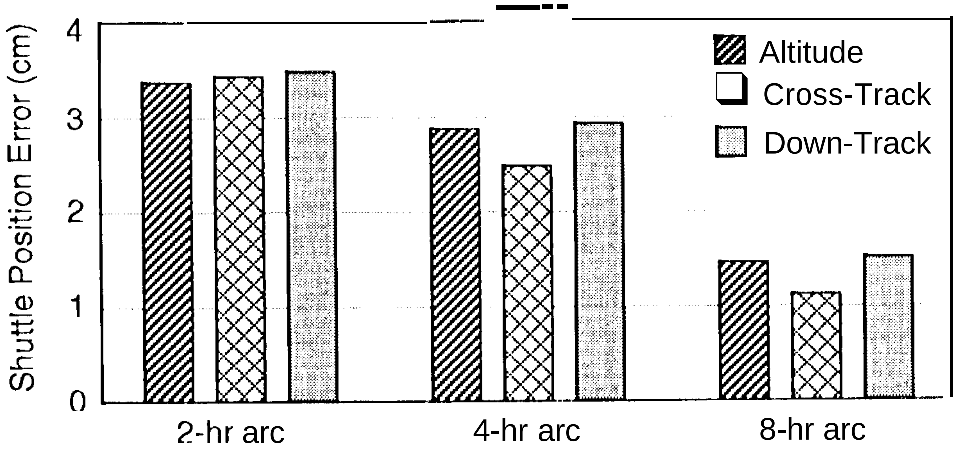

Fig. 17 Predicted Error for the Space Shuttle viewing all possible GPS within a sphere

JGM-1 Dynamic - Reduced Dynamic

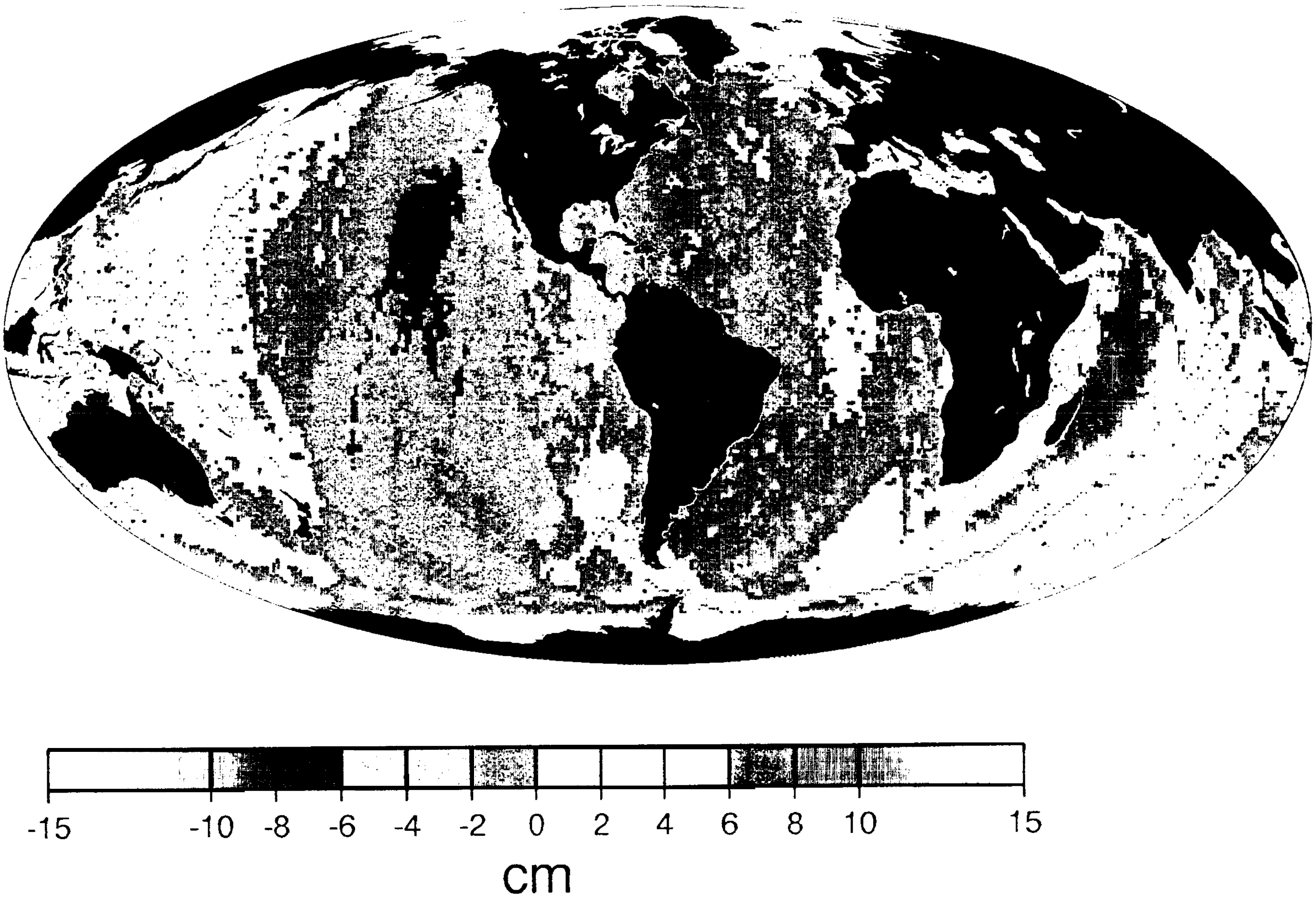

Plate I. (a)

JGM-1 Dynamic - JGM-2 Dynamic

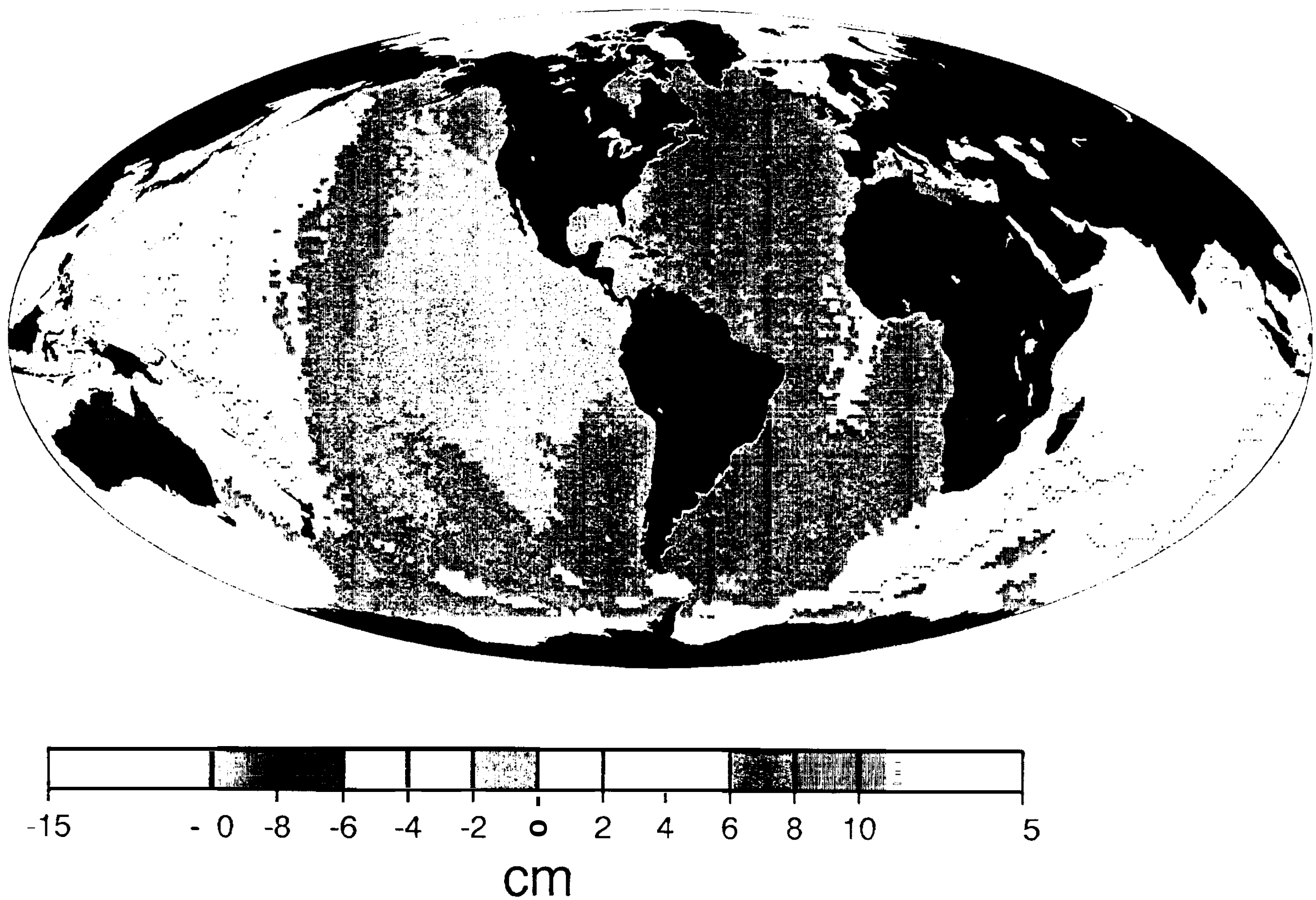

Plate 1. (b)

JGM-2 Dynamic - Reduced Dynamic

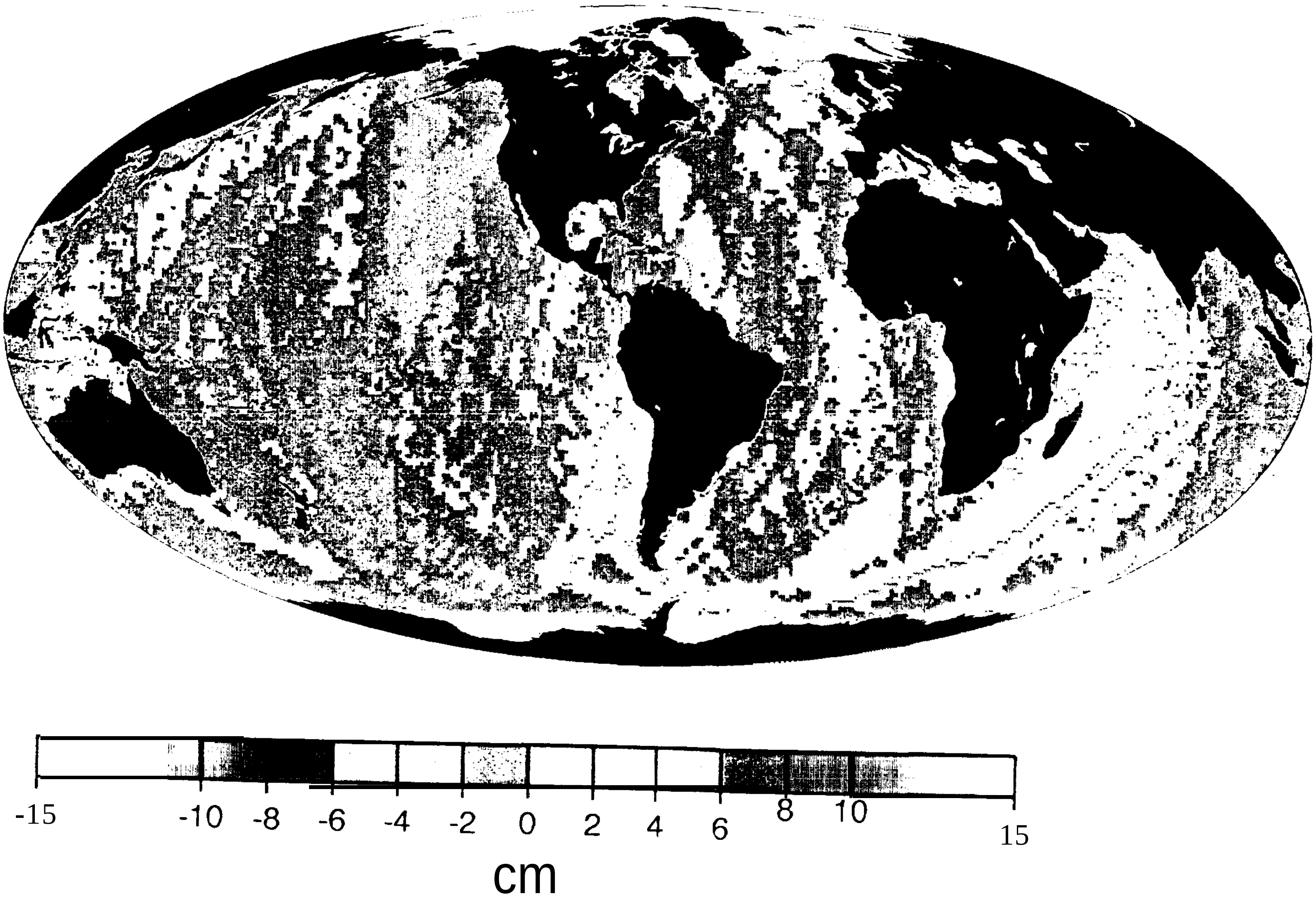

Plate 1. (c)